



**NAVAL  
POSTGRADUATE  
SCHOOL**

**MONTEREY, CALIFORNIA**

**THESIS**

**AIRBORNE HYPERSPECTRAL AND SATELLITE  
MULTISPECTRAL IMAGERY OF THE  
MISSISSIPPI GULF COAST REGION**

by

Lars O. Lone

December 2006

Thesis Advisor:  
Second Reader:

Robin Tokmakian  
Rost Parsons

**Approved for public release; distribution is unlimited**

THIS PAGE INTENTIONALLY LEFT BLANK

|   |   |  |  |  |
|---|---|--|--|--|
| <b>REPORT DOCUMENTATION PAGE</b>  |   |  | Form Approved OMB No. 0704-0188                            |  |
| Public reporting burden for this collection of information is estimated to average 1 hour per response, including the time for reviewing instruction, searching existing data sources, gathering and maintaining the data needed, and completing and reviewing the collection of information. Send comments regarding this burden estimate or any other aspect of this collection of information, including suggestions for reducing this burden, to Washington headquarters Services, Directorate for Information Operations and Reports, 1215 Jefferson Davis Highway, Suite 1204, Arlington, VA 22202-4302, and to the Office of Management and Budget, Paperwork Reduction Project (0704-0188) Washington DC 20503.   |   |  |  |  |
| <b>1. AGENCY USE ONLY (Leave blank)</b>   |   | <b>2. REPORT DATE</b><br>December 2006                         | <b>3. REPORT TYPE AND DATES COVERED</b><br>Master's Thesis |  |
| <b>4. TITLE AND SUBTITLE</b> Airborne Hyperspectral and Satellite Multispectral Imagery of the Mississippi Gulf Coast Region  |   |  | <b>5. FUNDING NUMBERS</b>                                  |  |
| <b>6. AUTHOR</b> LT Lars O. Lone  |   |  |  |  |
| <b>7. PERFORMING ORGANIZATION NAME AND ADDRESS</b><br>Naval Postgraduate School<br>Monterey, CA 93943-5000  |   |  | <b>8. PERFORMING ORGANIZATION REPORT NUMBER</b>            |  |
| <b>9. SPONSORING /MONITORING AGENCY NAME(S) AND ADDRESS(ES)</b><br>N/A  |   |  | <b>10. SPONSORING/MONITORING AGENCY REPORT NUMBER</b>      |  |
| <b>11. SUPPLEMENTARY NOTES</b> The views expressed in this thesis are those of the author and do not reflect the official policy or position of the Department of Defense or the U.S. Government.   |   |  |  |  |
| <b>12a. DISTRIBUTION / AVAILABILITY STATEMENT</b><br>Approved for public release; distribution is unlimited.  |   |  | <b>12b. DISTRIBUTION CODE</b>                              |  |
| <b>13. ABSTRACT</b><br><p>The Compact Airborne Spectrographic Imager (CASI) and the satellite Moderate Resolution Imaging Spectroradiometer (MODIS) provide detailed information about the environment U.S. Naval forces choose to operate. In recent years environmental conditions have been a driving factor in preventing the detection of underwater objects like mines. Suspended sediments are an environmental condition of interest. Remote sensors provide an opportunity to detect suspended sediments in a region prior to the commencement of operations and better prepare the force while reducing time required to complete operations.</p> <p>Monthly data sets collected using MODIS, from February 2005 to February 2006 show variations in weather patterns in the Mississippi Bight that cause the persistent presence of suspended sediments in certain areas of the Mississippi Bight. Major storm events such as hurricanes alter the location that suspended sediments persist in this region during hurricane season. MODIS with 250m-pixel resolution is capable of detecting large-scale suspended sediment plumes while CASI with 1m-pixel resolution is capable of detecting very fine suspended sediment filaments as well as provide early warning of possible mine locations.</p> <p>As the mine warfare fleet diminishes in size, CASI and MODIS coupled with current sensors may provide an increase in detection capability while reducing the workload of the ships. Continued research and study of suspended sediment transport during hurricane seasons would provide more information about how the environment changes.</p> |   |  |  |  |
| <b>14. SUBJECT TERMS</b> Multispectral imagery, Hyperspectral imagery, Suspended Sediments, MODIS, CASI, USW  |   |  | <b>15. NUMBER OF PAGES</b> 93                              |  |
|   |   |  | <b>16. PRICE CODE</b>                                      |  |
| <b>17. SECURITY CLASSIFICATION OF REPORT</b><br>Unclassified  | <b>18. SECURITY CLASSIFICATION OF THIS PAGE</b><br>Unclassified | <b>19. SECURITY CLASSIFICATION OF ABSTRACT</b><br>Unclassified | <b>20. LIMITATION OF ABSTRACT</b><br>UL                    |  |

THIS PAGE INTENTIONALLY LEFT BLANK

**Approved for public release; distribution is unlimited**

**AIRBORNE HYPERSPECTRAL AND SATELLITE MULTISPECTRAL IMAGERY  
OF THE MISSISSIPPI GULF COAST REGION**

Lars O. Lone  
Lieutenant, United States Navy  
B.S., Maine Maritime Academy, 2000

Submitted in partial fulfillment of the  
requirements for the degree of

**MASTER OF SCIENCE IN PHYSICAL OCEANOGRAPHY**

from the

**NAVAL POSTGRADUATE SCHOOL  
December 2006**

Author: Lars O. Lone

Approved by: Robin Tokmakian  
Thesis Advisor

Rost Parsons  
Second Reader

Mary Batteen  
Chair, Department of Oceanography

Donald P. Brutzman  
Chair, Undersea Warfare Academic Committee

THIS PAGE INTENTIONALLY LEFT BLANK

## **ABSTRACT**

The Compact Airborne Spectrographic Imager (CASI) and the satellite Moderate Resolution Imaging Spectroradiometer (MODIS) provide detailed information about the environment U.S. Naval forces choose to operate in. In recent years environmental conditions have been a driving factor in preventing the detection of underwater objects like mines. Suspended sediments are an environmental condition of interest. Remote sensors provide an opportunity to detect suspended sediments in a region prior to the commencement of operations and better prepare the force while reducing time required to complete operations.

Monthly data sets collected using MODIS, from February 2005 to February 2006 show variations in weather patterns in the Mississippi Bight that cause the persistent presence of suspended sediments in certain areas of the Mississippi Bight. Major storm events such as hurricanes alter the location that suspended sediments persist in this region during the hurricane season. MODIS with 250m-pixel resolution is capable of detecting large-scale suspended sediment plumes while CASI with 1m-pixel resolution is capable of detecting very fine suspended sediment filaments as well as providing early warning of possible mine locations.

As the mine warfare fleet diminishes in size, CASI and MODIS coupled with current sensors may provide an increase in detection capability while reducing the workload of mine detection ships. Continued research and study of suspended sediment transport during hurricane seasons may provide more information about how the environment changes.

THIS PAGE INTENTIONALLY LEFT BLANK



## TABLE OF CONTENTS

|      |   |    |
|------|---|----|
| I.   | INTRODUCTION.....   | 1  |
| A.   | BACKGROUND.....   | 1  |
| B.   | HISTORY.....  | 3  |
| C.   | MOTIVATION.....   | 5  |
| II.  | THEORY.....   | 9  |
| A.   | INHERENT AND APPARENT OCEAN OPTICAL PROPERTIES....                        | 11 |
| B.   | RADIATIVE TRANSFER EQUATIONS.....   | 13 |
| III. | DATA.....   | 21 |
| A.   | AIRBORNE HYPERSPECTRAL MEASUREMENTS.....                                  | 22 |
| 1.   | Bands Used.....   | 25 |
| 2.   | Data Sets.....  | 25 |
| B.   | SATELLITE MULTISPECTRAL MEASUREMENTS.....                                 | 27 |
| 1.   | MODIS Bands Used.....   | 29 |
| 2.   | MODIS Data Sets Used.....   | 30 |
| C.   | OTHER DATA SETS ACQUIRED.....   | 32 |
| 1.   | Wind Data.....  | 32 |
| 2.   | Current Data.....   | 33 |
| IV.  | PROCEDURES.....   | 35 |
| A.   | AIRBORNE HYPERSPECTRAL DATA COLLECTION,<br>PROCESSING, AND SCREENING..... | 35 |
| B.   | SATELLITE DATA COLLECTION, PROCESSING, AND<br>SCREENING.....              | 36 |
| C.   | STATISTICAL ANALYSIS.....   | 41 |
| 1.   | MODIS Statistical Analysis.....   | 42 |
| 2.   | CASI Statistical Analysis.....  | 44 |
| D.   | DATA COMPARISON.....  | 44 |
| V.   | RESULTS.....  | 47 |
| A.   | HYPERSPECTRAL IMAGERY ANALYSIS.....                                       | 48 |
| B.   | MULTISPECTRAL IMAGERY ANALYSIS.....                                       | 51 |
| 1.   | Yearly Multispectral Comparisons.....                                     | 51 |
| 2.   | Monthly Multispectral Imagery Comparison.....                             | 57 |
| 3.   | MODIS Suspended Sediment Assessment.....                                  | 60 |
| 4.   | Wind and Surface Current Evaluation.....                                  | 63 |
| C.   | AIRBORNE VS. SATELLITE COMPARISON.....                                    | 66 |
| VI.  | CONCLUSIONS AND RECOMMENDATIONS.....                                      | 69 |
| A.   | CONCLUSIONS.....  | 69 |
| B.   | RECOMMENDATIONS.....  | 71 |
| C.   | SUGGESTIONS FOR FUTURE STUDY.....   | 72 |
|      | LIST OF REFERENCES.....   | 73 |
|      | INITIAL DISTRIBUTION LIST.....  | 77 |

THIS PAGE INTENTIONALLY LEFT BLANK

## LIST OF FIGURES

|            |  |    |
|------------|--|----|
| Figure 1.  | Mississippi Bight region of interest displayed at 250m-pixel resolution. ....  | 7  |
| Figure 2.  | Electromagnetic energy observed by a remote sensor. Picture from OC3522 Remote Sensing, NPS. ....  | 12 |
| Figure 3.  | Flow chart for altering remotely sensed data (Lee et. al. 2002). ....  | 15 |
| Figure 4.  | CASI Push broom Sensor Operation (Smith et. al. 2000). ....  | 25 |
| Figure 5.  | Mississippi Barrier Islands are the locations for gathering hyperspectral imagery post Hurricane Katrina<br><a href="http://nationalatlas.gov/natlas/Natlasstart.asp">http://nationalatlas.gov/natlas/Natlasstart.asp</a><br>..... | 26 |
| Figure 6.  | NDBC buoy locations: <a href="http://mob.ndbc.noaa.gov">http://mob.ndbc.noaa.gov</a> . .   | 33 |
| Figure 7.  | Useable data per pixel for January 2005 to April 2005. ....  | 39 |
| Figure 8.  | Useable data per pixel for August 2005 through November 2005. ....   | 40 |
| Figure 9.  | Useable data per pixel for January 2006 through April 2006. ....   | 41 |
| Figure 10. | Daily versus monthly averaged absorption values for MODIS. ....  | 44 |
| Figure 11. | Data evaluation overview showing locations of data set analysis. ....  | 48 |
| Figure 12. | CASI True color hyperspectral image of the east side of Dauphin Island (1 m resolution). ....  | 49 |
| Figure 13. | MODIS true color multispectral image of all Mississippi Barrier Islands (250 m resolution)<br><a href="http://www7333.nrlssc.navy.mil/">http://www7333.nrlssc.navy.mil/</a> .....  | 49 |
| Figure 14. | Cat Island after Hurricane Katrina. Image taken by CASI November 29, 2005. ....  | 50 |
| Figure 15. | January to April 2005 monthly reflectance averages. ....   | 52 |
| Figure 16. | January to April 2006 monthly reflectance averages. ....   | 53 |
| Figure 17. | Yearly total absorption for three longitude lines for January months. ....   | 54 |
| Figure 18. | Yearly total absorption for three longitude lines for February months. ....  | 55 |
| Figure 19. | Yearly total absorption for three longitude lines for March months. ....   | 56 |

|            |  |    |
|------------|--|----|
| Figure 20. | Yearly total absorption for three longitude lines for April months. ....   | 56 |
| Figure 21. | August to November 2006 monthly reflectance averages. ....   | 58 |
| Figure 22. | Monthly total absorption for three longitude lines from August to November 2005. ....  | 59 |
| Figure 23. | Monthly zonal total absorption from August to November 2005. ....  | 60 |
| Figure 24. | January to April 2005 suspended sediment concentrations in the Mississippi Bight region.   | 61 |
| Figure 25. | August to November 2005 suspended sediment concentrations in the Mississippi Bight region.   | 62 |
| Figure 26. | January to April 2006 suspended sediment concentrations in the Mississippi Bight region.   | 63 |
| Figure 27. | Time series of daily wind speeds for buoy 42040. ....  | 64 |
| Figure 28. | Single point time series comparison of monthly total absorption to wind speed. ....  | 65 |
| Figure 29. | Four quarter surface current averages. <a href="http://oceancurrents.rsmas.miami.edu/">http://oceancurrents.rsmas.miami.edu/</a> ....                        | 66 |
| Figure 30. | October 2005 comparison of normalized absorption values of a meridional transect of satellite multispectral imagery and airborne hyperspectral imagery. .... | 67 |

## LIST OF TABLES

|          |  |    |
|----------|--|----|
| Table 1. | Symbols and Definitions for Radiative Transfer Equations (Lee et. al. 2002) .....  | 17 |
| Table 2. | List of Hurricanes and Tropical Storms making landfall in Gulf Coast region of the U.S. ....   | 22 |
| Table 3. | CASI Capabilities<br>( <a href="http://arsf.nerc.ac.uk/documents/casi2.pdf">http://arsf.nerc.ac.uk/documents/casi2.pdf</a> ) . . .   | 23 |
| Table 4. | CASI Operating Modes<br>( <a href="http://arsf.nerc.ac.uk/documents/casi2.pdf">http://arsf.nerc.ac.uk/documents/casi2.pdf</a> ) . . .  | 24 |
| Table 5. | CASI Data Sets Collected. ....   | 27 |
| Table 6. | MODIS Satellite Details<br>( <a href="http://modis.gsfc.nasa.gov/">http://modis.gsfc.nasa.gov/</a> ) . ....  | 28 |
| Table 7. | MODIS Technical Specifications<br>( <a href="http://picasso.coas.oregonstate.edu/ORS00/MODIS/code/MODP.pdf">http://picasso.coas.oregonstate.edu/ORS00/MODIS/code/MODP.pdf</a> ) .....                                  | 28 |
| Table 8. | MODIS two primary bands used to resolve 250 m pixel resolution<br>( <a href="http://picasso.coas.oregonstate.edu/ORS00/MODIS/code/MODP.pdf">http://picasso.coas.oregonstate.edu/ORS00/MODIS/code/MODP.pdf</a> ) . .... | 30 |
| Table 9. | MODIS Data Set Information .....   | 31 |

THIS PAGE INTENTIONALLY LEFT BLANK

## ACKNOWLEDGMENTS

First, I would like to thank my advisor, Robin Tokmakian of the Oceanography Department, for her help, guidance, and direction. Her perseverance and patience helped in the progress of this thesis.

Furthermore, I would like to express my gratitude to the personnel working at Naval Research Lab Stennis Space Center's Ocean Color Team: Rost Parsons as my second reader, Alan Weidemann, Bob Arnone, Brandon Casey and Sherwin Ladner. Their willingness to assist me is a testament to the capabilities they possess.

Also, thanks to the U.S. Army Corps of Engineers Mobile District in Kiln, MS: Jeff Lillycrop, Mary Whittington and Jennifer Wozencraft for providing a hyperspectral imagery set on very short notice. Their readiness and enthusiasm to aid my studies provided me the possibility to follow this thesis track.

Further, I would like to show appreciation to my Father, Mother, Karsten, Amalie and Linnea, my family who consistently provided support through humor, motivation and encouragement. You truly are precious to me.

Finally, I would like to thank Jerry Kim for pushing me to press on and spiritual uplifting, Preston and Jennifer Roland for providing food on the long days at school, and Josh Kiihne for aiding in stress relief at the firing range during the whole process.

THIS PAGE INTENTIONALLY LEFT BLANK



## **I. INTRODUCTION**

### **A. BACKGROUND**

In the global war on terror, mines have become an increasing threat due to the relative ease of making and affordability of purchasing these weapons. As always, timely, accurate, and detailed environmental data is needed to support the men and women in combat who may encounter these mines. As technology advances and new sensors become available new methods and analysis must be implemented to ensure systems are providing useful information in a suitable time to the war-fighter. The focus of this thesis is on using hyperspectral imagery and multispectral imagery sets to determine sediment loads in coastal regions after major storm events such as a hurricane. This will aid in the detection of mines as well as providing an estimate on conditions that may aid or hinder mine countermeasure operations.

The ocean has always been vitally important to the United States. The ability to exploit the ocean's environment for strategic advantage over enemies has always been a goal. The Naval Research Laboratory (NRL) at Stennis Space Center in Mississippi is at the Navy's forefront for providing detailed data related to underwater visibility. High frequency sonar systems are presently employed by United States forces to detect and classify mine like objects in ocean environments. These high frequency sonar systems give the user more ability to identify mines from trash on the ocean floor or in the water column, aiding in detection. The high frequency

sonar systems are prone to energy loss due to scattering and absorption by particulate matter in the water, much more so than lower frequency sonar's used to detect submarines. This nature is typical of light traveling through water as well.

Satellites are capable of detecting light that is reflected, emitted and scattered from the earth's surface, or near the surface by the sun. When sunlight hits the ocean's surface approximately two percent is reflected (Museler, 2003). The other ninety-eight percent enters the ocean and is absorbed, scattered, or reflected by particles in the water column. The energy that is reflected or emitted back to the atmosphere after entering the water column can be detected in the visible band of light by remote sensors and is known as water leaving radiance.

Measurements made by the Moderate Resolution Imaging Spectroradiometer (MODIS) satellites Terra and Aqua (managed and built by NASA) can be used to estimate many different ocean parameters such as sediment loads to chlorophyll content. This information, though very useful in showing large-scale relationships does not have a high enough resolution to view small-scale, localized events ranging in size from 100 meters to 1000 meters. This is because MODIS has a limited number of frequency bands that it can operate in. MODIS has 36 frequency bands, and of this only eight are used for ocean color imaging. Furthermore, for 250m-pixel resolution (highest resolution capable by MODIS) only 2 bands are used.

Hyperspectral imagers collect image data in many adjacent spectral bands simultaneously. The number of

bands can range from a couple dozen to several hundred. This process, explained by Smith (2006), derives a continuous spectrum for every imaged cell, resulting in much higher image resolution. Hyperspectral imagery taken by the U.S. Army Corps of Engineers (USACE) in Kiln, Mississippi was taken in the aftermath of Hurricane Katrina to determine the extent of damage done by the destructive storm. This higher resolution capability was used to survey damage to buildings and vegetation on the Mississippi Barrier Islands. Can this capability also be used to survey damage to the ocean environment? Can this information be exploited and provide information for the on-scene forces? An airplane flown at an altitude much closer to the earth than a satellite took the higher resolution imagery used in this thesis. Satellite hyperspectral imagers such as Earth Observer One (EO-1) have been tested and launched but are used to examine land features and not ocean effects (<http://eo1.gsfc.nasa.gov>).

## **B. HISTORY**

Museler (2003) showed that remote sensing has been used for fifty years now by several military branches and civilians. Buoys and airplanes accomplished early remote sensing of the ocean. As time progressed and technology advanced, satellites were launched to observe the earth from a distance. Satellite remote sensors provide more continuous global coverage than any other remote sensor. Ships, buoys, and airplanes combined cannot cover daily as much area as satellites can. These sensors give opportunity to study events long term. Ships and buoys can stay at sea for extended periods of time but only provide information about a small area. Airplanes can cover larger amounts of

area but are limited by the amount of fuel it can carry. Satellites are the only means of getting long-term, wide area coverage data.

MODIS satellite's Terra and Aqua were launched in 2000 and 2002 respectively. The Terra satellite has been deployed so that it travels from north to south across the equator in the morning while, the Aqua satellite travels from south to north across the equator in the afternoon. Terra received its name because its primary mission is to provide information on the status of land based Earth and its ecosystems. Aqua got its name because its name because its primary mission is to study the ocean based multidisciplinary nature of earth's interrelated processes. These processes include oceans, atmosphere and land interactions. These satellites allow near-real time analysis of the earth. Since their launch, the Naval Research Lab at Stennis Space Center (NRLSSC) has been providing data and imagery sets to the United States Military forces in several regions including areas naval forces cannot transect because of treaties and laws. Imagery sets include true-color images, and derived quantities such as chlorophyll concentrations, sea surface temperature (SST), total absorption, backscattering, color dissolved organic material (CDOM), and many others. Regions of interest to NRLSSC include the Gulf of Mexico, Mississippi, Eastern Pacific, Arabian Sea, Persian Gulf, Mediterranean Sea, Adriatic Sea and many others.

Hyperspectral imagery is a much newer data collection technique. First developed around 1990, the imagers were too bulky for use on satellites. Also, data storage and

transfer limitations prevented prolonged data collection with these types of imagers. After extensive testing in 2000, EO-1 was launched on a Delta 7320 from Vandenberg Air Force Base on November 21, 2000. It was inserted into a 705 km circular (438 mile), sun-synchronous orbit at a 98.7 degrees inclination. EO-1's primary purpose is to focus is to develop and test a set of advanced technology land imaging instruments (<http://eo1.gsfc.nasa.gov/>). Currently, there are not any hyperspectral imagers on U.S. satellites observing ocean features and the first imager is scheduled for launch in 2010. The Compact Airborne Spectrographic Imager (CASI) is the hyperspectral imager used by the Army Corps of Engineers. Mounted on an airplane, it is a system currently being used to find land mines in many regions such as Iraq and North Africa. Hyperspectral imagery is also being used to map coastlines and survey damage after natural disasters as with the case of Hurricane Katrina.

### **C. MOTIVATION**

No one area of remote sensing has had as much impact on environmental studies as imaging spectrometry (Smith et. al., 2000). Imaging is so important because of its ability to be manipulated and altered to enhance specific parameters such as suspended sediment content. Mines are subject to the environment in which they reside. The ability to detect them diminishes as suspended sediment concentrations increase due to scattering of the sonar source energy. Suspended sediment concentrations vary drastically as well due to many factors including storms and varying outflow from rivers. Certain bottom mines can also move into new locations by strong weather events and wave action.

As the Navy progresses towards littoral combat, the likelihood of encountering mines in shallow coastal waters increases. Coastal waters are often characterized by large concentrations of suspended sediment from river discharge or suspension from tides and waves (Miller and McKee, 2004). High-resolution imagery of near coastal regions is necessary to ensure battle space dominance and reduce the chance of damage to friendly forces. Miller and McKee also points out that the distribution of sediments is highly variable in coastal regions (Miller and McKee, 2004). This necessitates the need for long-term study and analysis of areas of interest on regional and daily to seasonal periods. It is advantageous to a range of environmental disciplines to develop better remote sensing approaches to determine sediment distribution because it could provide rapid quantitative synoptic data (Rainey et. al., 2003).

The Mississippi Bight is an ideal location to study variability of suspended sediment distribution for many reasons. It consists of many varying regions, such as the Mississippi River Delta and Mississippi Sound, which is protected by barrier islands. It is a region susceptible to major storm systems as well. The Mississippi Bight is also in U.S. territorial waters allowing in situ data to be gathered to compare to remotely sensed data. Figure (1) depicts the region of interest for this study.

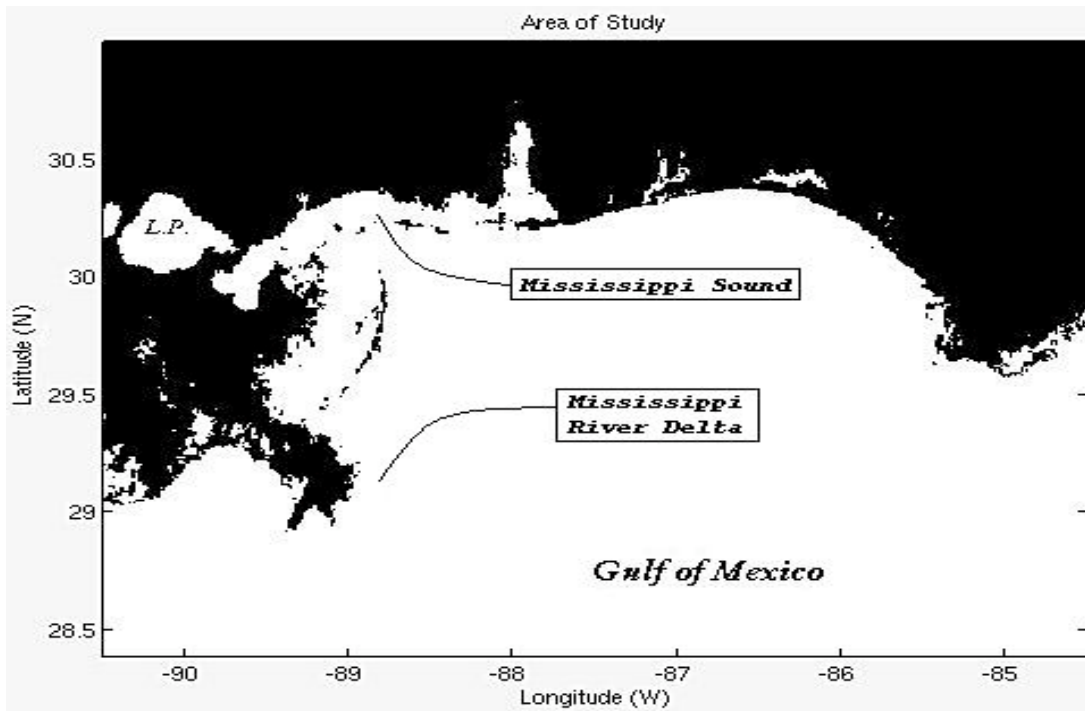


Figure 1. Mississippi Bight region of interest displayed at 250m-pixel resolution.

Miller and McKee (2004) showed that turbidity plumes can be observed and mapped using 250m-resolution satellite imagery. However, it is not high enough resolution to depict fully the dynamics of smaller bodies of water such as river inlets, estuaries and bays. Hyperspectral imagery can provide the necessary higher resolution capability to focus closer to shore in regions more likely to be traveled by U.S. Forces. Limitations on airspace, however, are still a concern in using any airborne imaging system.

Mapping seasonal changes in sediment transport is not a new concept. Ruhl et. al.(2001) looked at suspended sediment concentrations in the San Francisco Bay in California to determine transport; evaluating seasonal winds, spring and neap cycle, fresh water flow and semidiurnal tides to help explain the suspended sediment

travel. Likewise, Miller and McKee (2004) stated "distribution and flux of suspended sediments are highly variable over a broad spectrum of time and space scales." It is therefore very important to look at suspended sediment changes in both a monthly variation and yearly variation. This variation may provide valuable information to on scene commanders and others who may employ an area of operation.



## II. THEORY

Radiative transfer theory is the foundation for understanding and using remote sensors for detection of substances in the oceans. Museler (2003) defined it as the quantitative study, on a phenomenological level, of the transfer of radiant energy through media that absorbs, scatters or emits radiant energy. This transfer of energy can be through the atmosphere, or oceans. Both atmosphere and ocean environments must be considered when using remote sensors in orbit around the earth.

The sun gives off electromagnetic energy in a multitude of wavelengths but this study will focus only on the wavelengths that fall in the visible light band. Hyperspectral and multispectral imagers use wavelengths ranging from 390 nanometers (nm) to 740 nm. These bands are also in the visible light range for the human eye. The visible light band seen by the human eye derives ocean color, and color contains a wealth of information regarding composition and concentration of dissolved and suspended constituents in the sea (Roesler and Boss, 2002). Visible light wavelengths are very short as stated above. Suspended sediments range in size from 0.002mm to 0.06mm. This very small sediment size is still much greater than the wavelength of visible light that causes light to be reflected when it comes in contact with a sediment particle. Suspended sediments are best identified in the 530 nm range because of limiting interference from the atmosphere and ocean is at a minimum. At 500nm, energy interacts with atmospheric particles of 1-10 $\mu$ m size (Martin, 2004). The scattering is then strongly biased in the

return direction of the energy source. This is known as Mie Scattering (Martin, 2004).

The atmosphere plays an important role in determining what can be seen in the oceans. Airborne constituents such as clouds, aerosols, pollutants etc. affect what the sensor can detect in the oceans. Clouds in many instances hide physical objects beneath them preventing information from being gathered about the oceans contents. Aerosols and other pollutants are either a source of radiance or scatter visible energy making detection of the oceans contents much more difficult. Methods to remove these atmospheric effects and retrieve remotely sensed optical properties have been investigated for decades (Lee et. al., 2002).

Several oceanic processes prevent viewing of particulate matter in the ocean. Sun glint is a common occurrence on a smooth ocean surface or at low solar angles such as in the early morning or late afternoon. The strong reflection saturates an imaging sensor preventing useful information from being gathered. Another oceanic process that can affect data gathering information is breaking waves. Very strong winds in the open ocean cause waves to overturn entraining bubbles. The bubbles disrupt the sensors capability in much the same way that clouds disrupt the sensor. White caps can also be found near coastal regions where waves interact with the ocean floor. Other characteristics such as oil spills can also limit a passive sensors ability to observe the ocean environment.

A majority of satellite passive sensors do not look at nadir views (perpendicular to flight path) whereas airborne passive sensors do. Also, there is typically some angle of incidence at which the imager views. Significant errors

and distortions are introduced with large angles of incidence. This is a problem much more readily seen in airborne imagers, as they are closer to the earth than satellites. In both sensor types, mathematical geometric corrections must be applied to remove the distortion.

#### **A. INHERENT AND APPARENT OCEAN OPTICAL PROPERTIES**

Inherent optical properties are those properties that do not change based upon conditions that arise. The most notable is the attenuation coefficient ( $c$ ). Morel & Loisel (1998) state that the attenuation coefficient can be reduced to the sum of the volume scattering coefficient ( $b$ ), and the absorption coefficient ( $a$ ). It is also possible the energy is neither scattered nor absorbed by the water column and thus transmitted through the water column.

Understanding how passive, remote sensors work is key to analyzing data that they gather. Properties both inherent and apparent are seen in passive sensors. These are explained below in detail. Figure (2) provides a cartoon image depicting the apparent optical properties received by passive remote sensors such as MODIS and CASI. The cartoon shows interferences caused by all of the effects discussed above. Likewise, the cartoon is color-coded showing which bands of light are absorbed, scattered, and reflected by the ocean.

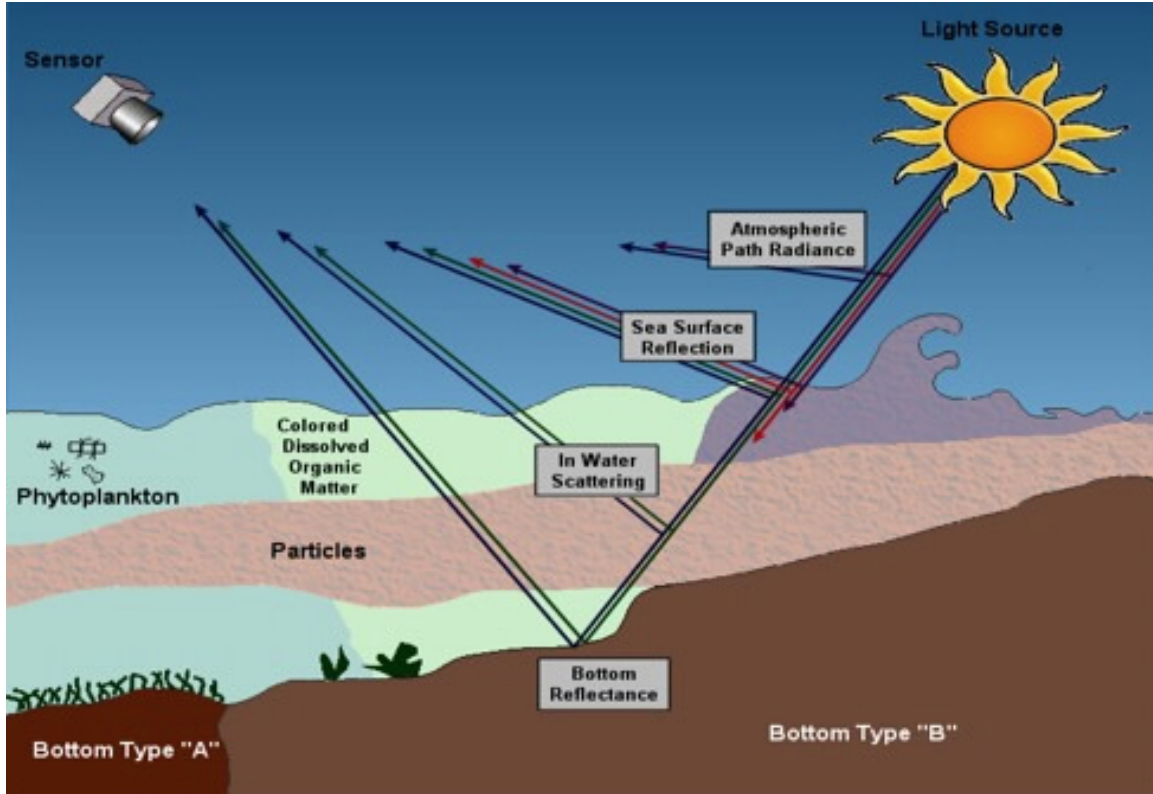


Figure 2. Electromagnetic energy observed by a remote sensor. Picture from OC3522 Remote Sensing, NPS.

Unlike inherent optical properties, apparent optical properties are affected by environmental conditions. In order to obtain valid results from remote sensors, atmospheric correction of the satellite data is necessary (Melin et. al., 2005). This is best shown through mathematical explanation that is shown below in this section. Most notable apparent optical changes are caused by the change in the amount of electromagnetic radiation received by the ocean from the sun. Passive sensors such as MODIS and CASI detect these apparent optical properties. In order to determine the inherent optical properties the two are related by:

$$\kappa \equiv a + b_b \quad (1)$$

where  $\kappa$  is the attenuation coefficient and  $b_b$  is the backscattering coefficient expanded as:

$$b_b(\lambda) = b_{bw}(\lambda) + b_{bp}(\lambda) \quad (2)$$

where  $b_{bw}$  is the backscattering coefficient of pure seawater,  $b_{bp}$  is the backscattering coefficient of suspended particles, and  $\lambda$  is a given wavelength band and  $a$  is expanded as:

$$a(\lambda) = a_w(\lambda) + \Delta a(\lambda), \quad (3)$$

where  $a_w$  is absorption coefficient for pure water and  $\Delta a$  is the contribution from dissolved or suspended matter. The radiative transfer equation is discussed more in the following section.

## **B. RADIATIVE TRANSFER EQUATIONS**

The Radiative Transfer Equations are the foundation for using remote sensing data sets. These equations describe how radiation passes through the atmosphere and ocean. Preisendorfer (1976) provides an equation for a simple radiative transfer model, which is:

$$\frac{dL}{dr} = -(a+b)L + L_o,$$

(4)

where  $L$  is the apparent radiance,  $L_o$  is the path function,  $r$  is the path distance,  $a$  is absorption and  $b$  is backscatter.

To solve the simple radiative transfer model several coefficients must be known such as the attenuation coefficient, radiance path, azimuth angle of the sun, and the path function. Satellites do not always pass over a region of interest at local apparent noon, nor are planes always capable of flying over a location with the sun

directly overhead. Empirical methods are used to expand equation (4) to get more accurate information. When the coefficients above are not known due to lack of in-situ sampling limitations, other methods are devised to estimate these values and reduce the equations to subsets which can be analyzed and are explained below.

There are four basic product levels available to the user. Each set involves a modification or derivation of the previous product. Levels 0-3 relate to the amount of mathematical analysis. This analysis can be done using empirical algorithms or by quasi-analytical algorithms (shown below). Empirical algorithms are experimental equations applied to aid in explanation of observed phenomenon. Empirical algorithms are limited in capability as they only provide information for case 1-water types, which have been observed significantly. They are primarily used for chlorophyll a concentrations. On the other hand, quasi-analytical algorithms use a combination of experimental equations but include running several models to determine values that fit data to curves. Quasi-analytical algorithms are used to determine other constituents such as Gelbstoff, absorption coefficient, colored dissolved organic matter (CDOM), bottom types, pigments and many others. Though more time consuming to use, quasi-analytical algorithms provide greater amounts of information over a wider range of water types. Figure 3 shows the method for applying quasi-analytical equations to data sets in order to obtain values of interest.

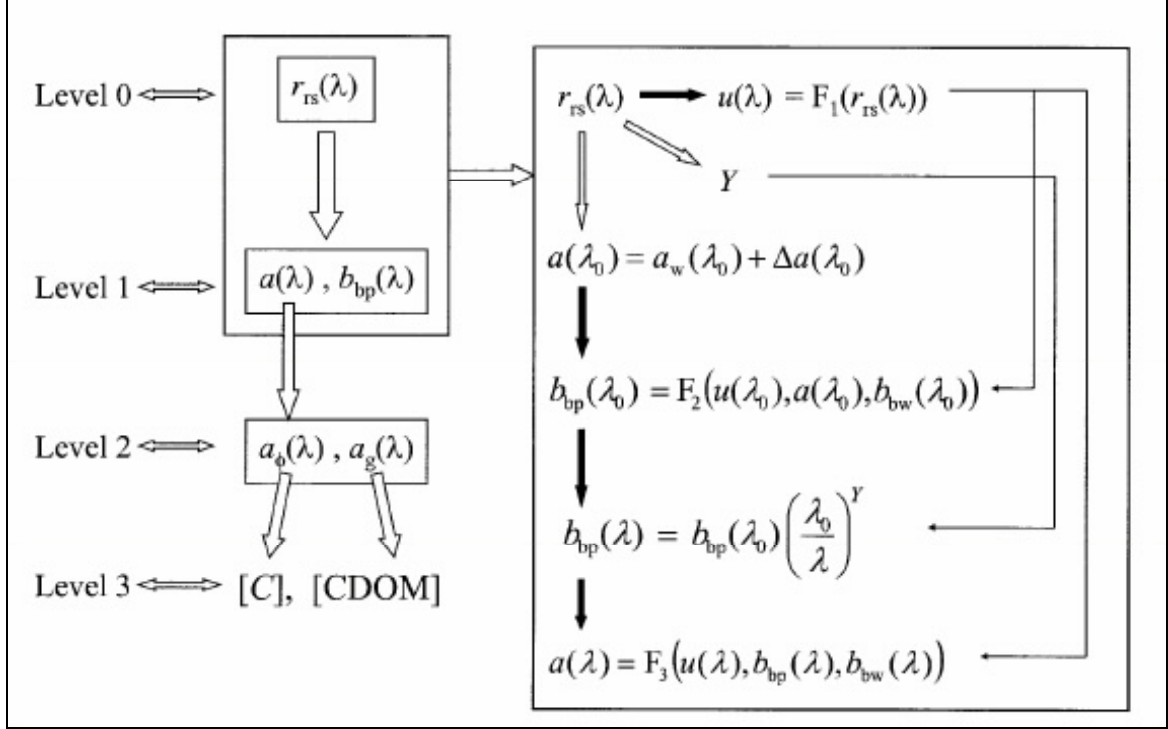


Figure 3. Flow chart for altering remotely sensed data (Lee et. al. 2002).

Level (0) products involve manipulation of the below-surface reflectance ( $r_{rs}$ ) using the ratio of backscattering coefficient to the sum of absorption and backscattering coefficients ( $u$ ) shown below:

$$r_{rs}(\lambda) = g_0 u(\lambda) + g_1 [u(\lambda)]^2, \quad (5)$$

where  $g_0$  and  $g_1$  are coefficients that vary from location to location. They are derived through a semi-analytical formula where  $g_0 = 0.084 + 0.11R$  and  $g_1 = 0.0794 + 0.0906R$  and  $R$  is a random number between zero and one. This approximates real world values for  $g_0$  and  $g_1$ . Since  $g_0$  and  $g_1$  are not known for all locations of the earth using remote sensors, Lee et. al. (2002) showed that adding a random variable and running a model over a region of interest approximates the real-world values with a high degree of accuracy.

In some instances the coefficient ( $u$ ) for a given wavelength may not be known but ( $r_{rs}$ ) for the same wavelength is known. ( $u$ ) is then determined using the quadratic formula in the equation shown below:

$$u(\lambda) = \frac{-g_0 + [(g_0)^2 + 4g_1 * r_{rs}(\lambda)]^{\frac{1}{2}}}{2g_1}, \quad (6)$$

which is another semi-analytical equation where values for the terms are the same as those shown in equation (5).

Backscattering of suspended particles can be calculated as shown in equation (2) but when certain constituents want to be viewed (such as suspended sediments) the equation for backscattering must be modified as:

$$b_{bp}(\lambda) = b_{bp}(\lambda_0) \left( \frac{\lambda_0}{\lambda} \right)^Y, \quad (7)$$

where wavelengths may be varied to view particular features using some reference wavelength ( $\lambda_0$ ). A typical value for  $\lambda_0$  is 440 nm. The spectral power ( $Y$ ) is determined by:

$$Y = -2.2 \{ 1 - 1.2e^{[-0.9 \frac{r_{rs}(\lambda_0)}{r_{rs}(\lambda)}]} \}, \quad (8)$$

where  $Y$  is either known or fairly easily measured from a remote sensor.

Level 2 products are computed by finding the values of absorption for phytoplankton ( $\alpha_\phi$ ) and Gelbstoff ( $\alpha_g$ ) and are dependent on wavelength. The equations are written as:

$$a_\phi(\lambda) = a(\lambda) - a_g(\lambda) - a_w(\lambda), \quad (9)$$

where attenuation value for the Gelbstoff coefficient is given by:



$$a_g(\lambda) = \frac{[a(\lambda) - \zeta a(\lambda)]}{\xi - \zeta} - \frac{[a_w(\lambda) - \zeta a_w(\lambda)]}{\xi - \zeta}, \quad (10)$$

where  $\xi = \alpha_\phi(410)/\alpha_\phi(440)$  and  $\zeta = \alpha_g(410)/\alpha_g(440)$ .

Level three products are varying combinations of level one and two. Data sets used in this study where level three products. NRLSCC and USACE computed all levels of modification. Table (1) below gives a description and quick reference for each term used in figure (4) above and the equations.

Table 1. Symbols and Definitions for Radiative Transfer Equations (Lee et. al. 2002)

| Symbol        | Description                                       | Units            |
|---------------|---|------------------|
| $\alpha$      | Absorption Coefficient                            | $\text{m}^{-1}$  |
| $\alpha_\phi$ | Absorption Coefficient of phytoplankton           | $\text{m}^{-1}$  |
| $\alpha_w$    | Absorption Coefficient of pure sea water          | $\text{m}^{-1}$  |
| $\alpha_g$    | Absorption Coefficient of Gelbstoff/Detritus      | $\text{m}^{-1}$  |
| $\lambda$     | Wavelength  | nm               |
| $\lambda_0$   | Reference wavelength                              | nm               |
| $b_{bp}$      | Backscattering Coefficient of Suspended Particles | $\text{m}^{-1}$  |
| $b_{bw}$      | Backscattering Coefficient of Pure Sea Water      | $\text{m}^{-1}$  |
| $b_b$         | Total Backscattering Coefficient                  | $\text{m}^{-1}$  |
| $R_{rs}$      | Above-surface Remote Reflectance                  | $\text{sr}^{-1}$ |
| $r_{rs}$      | Below-surface Remote Reflectance                  | $\text{sr}^{-1}$ |

|     |  |                  |
|-----|--|------------------|
| S   | Spectral Slope of Gelbstoff Absorption Coefficient   | nm <sup>-1</sup> |
| Y   | Spectral Power for Particle Backscattering Coefficient                                       | N/A              |
| u   | Ratio of Backscattering Coefficient to the Sum of Absorption and Backscattering Coefficients | Nm               |
| [C] | Pigment Concentrations   | N/A              |

High-frequency sonar is scattered by sediment and ultimately makes detection of mines harder. Kunte et. al. (2005) points out that suspended sediments ( $X_s$ ) can be derived from knowing  $a$  and reflectance ( $R$ ) by:

$$X_s = \frac{\frac{R(\lambda_1)}{R(\lambda_2)}}{\left(\frac{R(\lambda_3)}{R(\lambda_1)}\right)^{-0.5}} \quad (11)$$

where  $R(\lambda_1)$  is the wavelength that best reflects sediments typically around 550nm,  $R(\lambda_2)$  is a wavelength value greater than  $R(\lambda_1)$ , typically about 670 nm, and  $R(\lambda_3)$  is a wavelength value less than  $R(\lambda_1)$  and is typically around 490 nm. Using equation (11) may provide useful information to the end user in properly tuning a high-frequency sonar system prior to entering a mined region.

Light received by the sensor is reflected light. More light that is reflected from the ocean and detected by the sensor implies that less is being absorbed. Therefore, there must be more particulate matter in the water reflecting the sunlight. This is an important concept to

grasp when later figures are analyzed and is key to understanding information that is provided when using equation (11).

THIS PAGE INTENTIONALLY LEFT BLANK

### III. DATA

Images of water leaving radiance were taken in the Mississippi Bight region. The area of interest for satellite imagery is from  $28.5^{\circ}$  to  $31.0^{\circ}$  North Latitude and  $84.0^{\circ}$  to  $91.0^{\circ}$  West longitude, which can be seen in Figure (1). The airborne imagery is in the same region but due to its higher resolution capability and smaller aerial coverage the whole region is not sampled. The Mississippi Barrier Island chains are the focus in the hyperspectral imagery sets. They cover  $30^{\circ}11'24''\text{N}$  to  $30^{\circ}16'39''\text{N}$  Latitude and  $88^{\circ}03'\text{W}$  to  $88^{\circ}09'\text{W}$  longitude. The next sections describe the CASI data set and the MODIS satellite data in detail.

The time period used in this study covered a period of time leading up to the most violent hurricane season reported in history. This study then looks at the hurricane season in detail and finally the calm season following the 2005 hurricane season. Violent storms such as tropical storms and hurricanes can change a region drastically. Last year was no exception with damages exceeding \$100 billion, and a record setting twenty-eight storms were recorded with seven major storms hitting the Gulf-coast region. The table below lists provides more information about the storms that affected the region.

Table 2. List of Hurricanes and Tropical Storms making landfall in Gulf Coast region of the U.S.

| Storm Name | Date            | Storm Type/class  | Location Hit    |
|------------|-----------------|-------------------|-----------------|
| Arlene     | 8-13 June       | Tropical Storm    | Florida         |
| Cindy      | 3-7 July        | Tropical Storm    | Mississippi     |
| Dennis     | 4-13 July       | Hurricane (cl. 3) | Florida         |
| Katrina    | 23-31 August    | Hurricane (cl. 4) | Mississippi     |
| Rita       | 18-26 September | Hurricane (cl. 2) | Texas/Louisiana |
| Tammy      | 5-6 October     | Tropical Storm    | Florida         |
| Wilma      | 15-25 October   | Hurricane (cl. 3) | Florida         |

#### A. AIRBORNE HYPERSPECTRAL MEASUREMENTS

CASI is an instrument developed by ITRES Research Limited of Canada. It operates as a push-broom scanner, collecting imagery along a line at a time perpendicular to the aircraft motion (Smith et. al. 2000). As the airplane tracks along its course, an image is produced. CASI is a versatile instrument capable of being placed in many different types of airplanes and operated at altitudes ranging anywhere from approximately 1,000ft to 10,000ft. This said, the swath width is also variable ranging from 2nm to 12nm (<http://www.es.ucsc.edu/>). Table (3) provides more information on capabilities of the CASI Instrument. CASI can operate in full frame mode with 512 spatial pixels and 288 samples but data smearing may occur so compromises must be made to view data accurately (NERC ARSF, 2005). CASI's default settings are also set to view vegetation on landmasses. To look at ocean-specific traits, the settings need to be changed. Imagery from CASI must also be

evaluated after the mission has been flown because of the size of the imagery data sets.

Table 3. CASI instrument capabilities  
(<http://arsf.nerc.ac.uk/documents/casi2.pdf>).

| <b>IFOV (Instantaneous Field of View)</b> |                       |
|---|-----------------------|
| Across Track                              | 54.4 degrees          |
| Along Track                               | 0.1151 degrees        |
| Spectral range                            | 405-950 nm            |
| Spatial samples                           | 512 spatial pixels    |
| Spectral samples                          | 288 @ 1.8nm intervals |

CASI is also capable of operating in several different modes depending upon types of information that must be gathered. The two most common are spatial mode and spectral mode. Each of the modes has advantages and disadvantages. Spatial mode is limited by the number of bands but gives a spatially adjacent multi-band image because data is recorded from all 512 pixels. Spectral mode is limited in look angle using only thirty-nine of the pixel positions but can provide a detailed, high-resolution spectral profile. The enhanced spectral mode is similar to the spectral mode but resolution is reduced slightly to increase spatial coverage using 101 adjacent spatial pixels. The spectral modes are also limited by integration times and cannot be used at low altitudes without significant distortion. Full-frame mode is typically used for calibration of the instrument or if the imager is stationary observing stationary objects.

Table 4. CASI Operating Modes  
(<http://arsf.nerc.ac.uk/documents/casi2.pdf>).

| <b>Operating Modes</b> |  |
|------------------------|--|
| Spatial Mode           | 512 pixel, 18 spectral bands                                     |
| Spectral Mode          | Full spectrum (288 channels)                                     |
| Enhanced Spectral Mode | Full spectrum (288 channels)<br>in 101 adjacent spatial pixel    |
| Full Frame             | 512 pixels across by 288<br>spectral pixels (lab<br>calibration) |

Figure (4) below, provides an example of how the CASI imager operates as the airplane flies along a given path. It also gives a blown up view of how the spatial and spectral elements are aligned in order to gather the data. The aircraft should fly at a constant speed and constant altitude over the intended target to ensure that distortion is minimized.



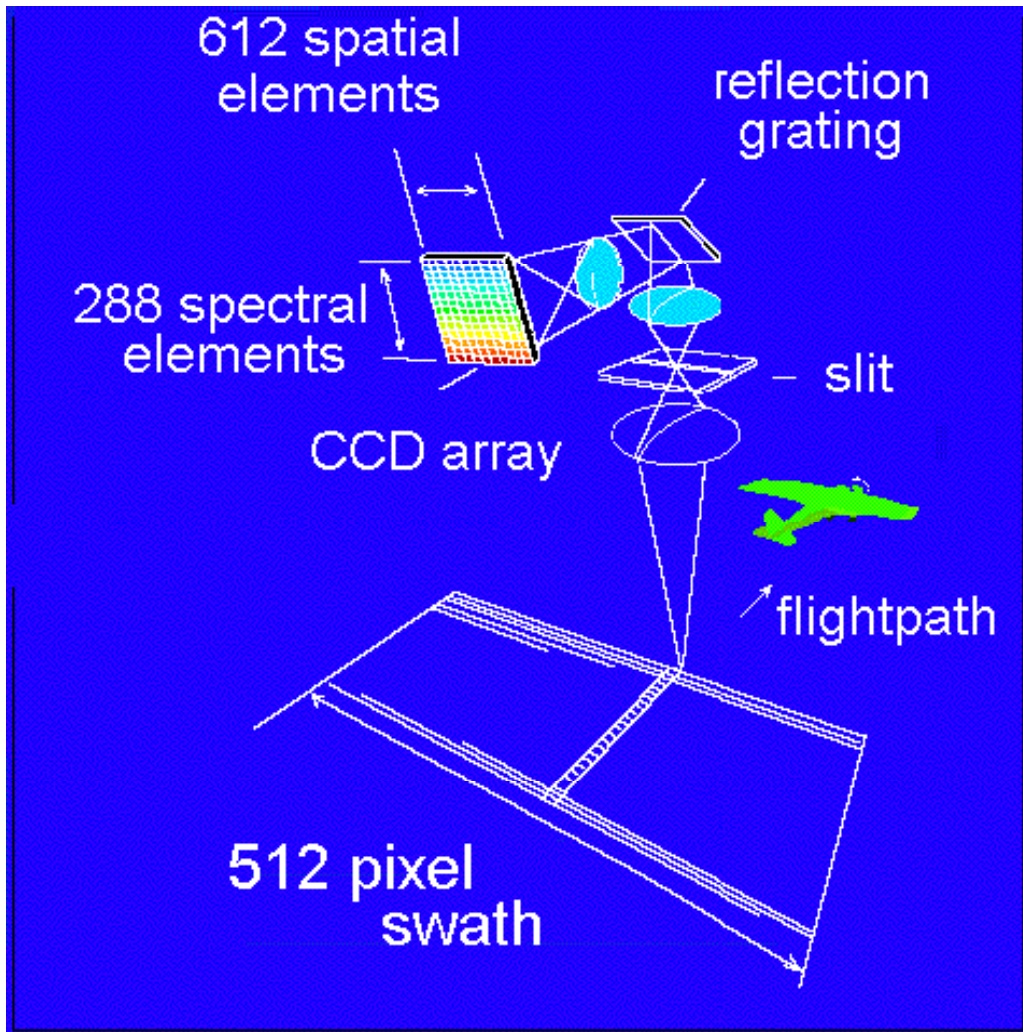


Figure 4. CASI Push-broom Sensor Operation (Smith et. al., 2000).

### 1. Bands Used

CASI was used in the Spatial Mode using 18 bands and 512-pixel swath. All eighteen bands create a true color image of the area covered. This true color image can be broken into individual bands and edited. Bands 5, 6, 7, 8, and 11 are optimal bands for determining sediment content.

### 2. Data Sets

The sample set evaluated in this study was small. It was comprised of 6 images. Each image covered individual

islands in the Mississippi Barrier Island region. The image below gives the location of the Mississippi Barrier Islands.

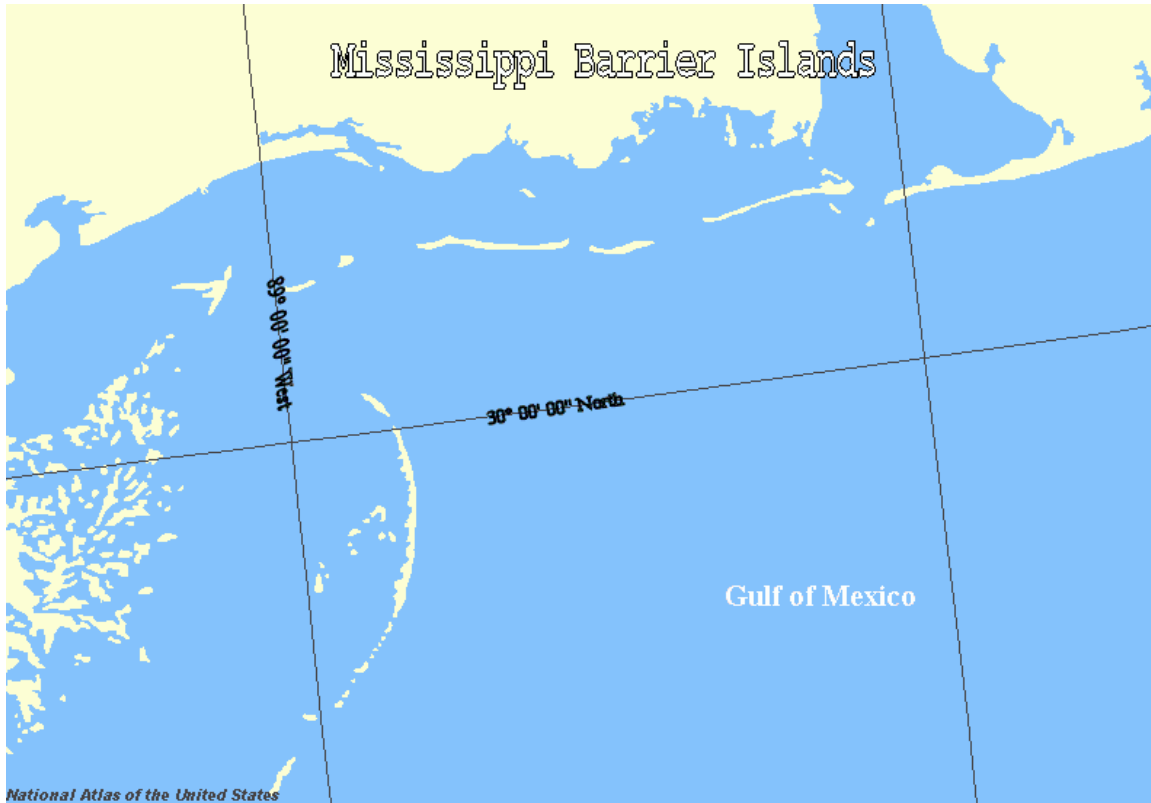


Figure 5. Mississippi Barrier Islands are the locations for gathering hyperspectral imagery following Hurricane Katrina (<http://nationalatlas.gov/natlas/Natlasstart.asp>, 2006)

More specifics are provided in the table below. All of the data was collected in 2005 after Hurricane Katrina hit the Mississippi Gulf Coast region. Half of the data was collected in October while the other half was collected in November. Flight limitations due to storm activity caused the sporadic data collection times.

Table 5. CASI Data Sets Collected.

| Month    | Day            | Time     | Island                 |
|----------|----------------|----------|------------------------|
| October  | Sunday, 30th   | 1439 CST | Ship                   |
|          | Monday, 31st   | 1515 CST | Horn                   |
|          | Monday, 31st   | 1531 CST | Petit Bois             |
| November | Wednesday, 2nd | 1727 CST | Dauphin (east)/Pelican |
|          | Tuesday, 22nd  | 1655 CST | Dauphin (west)         |
|          | Tuesday, 29th  | 1445 CST | Cat                    |

#### B. SATELLITE MULTISPECTRAL MEASUREMENTS

TERRA and AQUA satellites are both flying in low earth orbit (LEO) at approximately 438 miles. Terra satellite crosses the equator at approximately 10:30 Central Standard Time (CST) everyday while the Aqua satellite crosses the equator at 1:30 CST daily. Because of the timing, and sun-synchronous orbit, these two satellites provide nearly global coverage every one to two days and provide multiple looks at any given point on the earth. Multiple looks at a given area also reduce the level of uncertainty and error in data sets because more data is available for evaluation. Data is more meaningful statistically when there are more samples. More data also provides a higher degree of correlation in data sets. MODIS is only one of many sensors employed by Terra and Aqua satellites. More satellite details on which MODIS is employed are shown in Table (6).

Table 6. MODIS Satellite Details  
(<http://modis.gsfc.nasa.gov/>, 2006).

|              | <b>TERRA</b>   | <b>AQUA</b>  |
|--------------|--|--|
| Orbit height | 705 km (438 mi)  | 705 km (438 mi)  |
| Orbit type   | 10:30 am, descending,<br>sun-synchronous, near-<br>polar, circular | 1:30 pm, ascending,<br>sun-synchronous, near-<br>polar, circular |
| launch date  | Dec 18 1999  | May 04 2002  |

MODIS, like CASI is a push broom sensor. As Terra and Aqua travel along their respective paths, MODIS scans from side to side. Due to their altitudes, the swath is much larger than CASI'S. Information from MODIS is continually transferred to ground stations as well. This means data can be analyzed quickly, and near-real-time (twelve hours to forty-eight hours) information can be provided to naval forces. Spatial resolution is also adjustable depending on needs and the different settings are shown in Table (7). Table (7) provides amplifying technical information about the MODIS instrument.

Table 7. MODIS Technical Specifications  
(<http://picasso.coas.oregonstate.edu/ORSOO/MODIS/code/MODP.pdf>, 2006)

|                    |                          |
|--------------------|--------------------------|
| scan rate          | 20.3 rpm, cross track    |
| swath              | 2330 km x 10 km          |
| quantization       | 12 bits                  |
| data rate          | 10.6 Mbps (peak)         |
| spatial resolution | 250 m<br>500 m<br>1000 m |

Providing near-real-time data to forces allows commanders to make better informed decisions, preventing unnecessary losses of life or wasted time.

## 1. MODIS Bands Used

This study focused on using the highest spatial resolution (250m-pixel resolution) imagery MODIS provides. 250 m resolution imagery is provided from channels one and two. It can then be combined with other wavelengths to view specific characteristics such as total absorption. For this study, the wavelengths of interest are 488nm, 531nm, and 551nm total absorption values.

Channel one provides coverage in the red spectrum and is sensitive enough for use in coastal water studies (Miller and McKee 2004). Channel two provides coverage in the near Infra-red (NIR) spectrum. Combining these two channels allows clouds and other airborne aerosols to be removed from an image algorithmically. NIR is not affected by cloud cover as visible light is. By combining collocated MODIS IR clear radiance observations and cloudy radiance measurements, the clear column radiances can be retrieved by using the optimal cloud-clearing method (Li et. al., 2005). The optimal cloud-clearing method ( $N^*$ ) can be written as:

$$N^* = \frac{f(R_1(\lambda)) - R^c(\lambda)}{f(R_2(\lambda)) - R^c(\lambda)} \quad (15)$$

where  $f$  is the IR band for MODIS,  $R_i$  is the cloudy radiance value for a given footprint and wavelength, and  $R^c$  is the average clear radiance for a given wavelength (Li et. al., 2005).

The cloud-clearing method is applied to the radiance prior to completing level zero products to limit bias or errors in data sets. Below, in Table (7), the bands used are displayed in more detail. In some instances cloud

cover in particular pixels cannot be resolved using the method described. The particular pixel information may be corrupted in transmit between satellite and ground station, and another similar reason. In those cases, the pixel is given a value similar to that of land and mapped out entirely.

Table 8. MODIS two primary bands used to resolve 250 m pixel resolution  
(<http://picasso.coas.oregonstate.edu/ORSOO/MODIS/code/MODP.pdf>, 2006).

| Channel | Band (nm) [bandpass] | Spatial resolution |
|---------|----------------------|--------------------|
| 1       | 659 [50]             | 250 m              |
| 2       | 865 [35]             | 250 m              |

## 2. MODIS Data Sets Used

Due to MODIS' persistent pervasive presence, much more data was acquired and analyzed. Several months worth of data were collected. This data was separated by season and then separated by month. The seasonal focus is on the times that hurricanes are possible in the region and the times they are not. "Hurricane season" begins on June 1 and lasts until November 30. The Mississippi Bight region during 2005 saw a peak in hurricane activity between August and November. During the hurricane free season of 2005 and 2006 data from January to April were analyzed. Table (9) delineates concisely what data sets were used. These particular months were chosen for several reasons. First, January to April of 2005 is the winter to spring season prior to the exceptionally busy storm season of 2005. Using these months sets a baseline for absorption and sediments values. August to November 2005 are the busiest

months of the hurricane season resulting in three of the four hurricanes and one tropical storm that hit the region of interest. This comparison shows the variability. The final four months, of January to April 2006 will show changes in absorption and sediment levels from the baseline set by 2005 data.

Table 9. MODIS Data Set Information

| Month     | Year | Sample Size | Missing Days |
|-----------|------|-------------|--------------|
| January   | 2005 | 36          | 0            |
| February  | 2005 | 49          | 0            |
| March     | 2005 | 72          | 0            |
| April     | 2005 | 59          | 1            |
| August    | 2005 | 44          | 5            |
| September | 2005 | 67          | 0            |
| October   | 2005 | 67          | 5            |
| November  | 2005 | 63          | 2            |
| January   | 2006 | 54          | 0            |
| February  | 2006 | 34          | 0            |
| March     | 2006 | 14          | 17           |
| April     | 2006 | 16          | 13           |

Data sets vary in size between the months studied for various reasons. One major cause of data set size is the footprint of the MODIS sensor. It is not quite large enough to cover the entire earth at the equator. This

causes small gaps in information. Though these gaps move with time, data may not cover the region of interest thus limiting the data set size. Using two satellites further reduces the number of days missed, as gaps produced by Terra are not in the same location as those produced by Aqua. Significant cloud cover for multiple days can also limit sample size. For example, Hurricane Katrina stalled out over the Mississippi Gulf region causing the images to be significantly cloudy resulting in a period of time where no data available. Computer-server malfunctions at NRLSSC are another reason data sets can be limited in size and resulted in data being lost for post processing. Two months in particular where this loss can be seen is in March and April 2006 where sample sizes (measured in days per month) are in the high teens to low twenties. This is described in the following section of this thesis.

## **C. OTHER DATA SETS ACQUIRED**

### **1. Wind Data**

In situ wind data from the National Data Buoy Center (NDBC) was also extracted from <http://mob.ndbc.noaa.gov>. It was collected to aid in the explanation and understanding of the variability in the imagery's reflectance values. These data sets were collected from two specific buoys: 42007 at location 30.09<sup>0</sup> North Latitude and 88.77<sup>0</sup> West Longitude. Buoy 42040 is located at 29.18<sup>0</sup> North Latitude and 88.21<sup>0</sup> West Longitude. Both are shown in the image below.



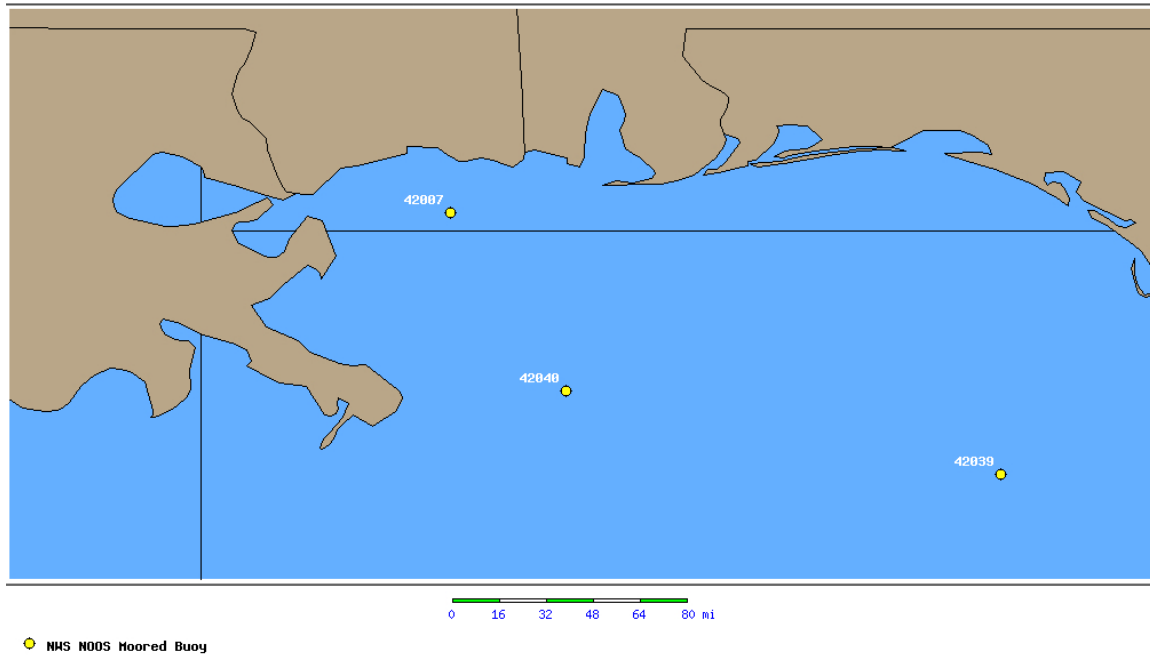


Figure 6. NDBC buoy locations: <http://mob.ndbc.noaa.gov>.

These two buoys were chosen because of their locations on and off shore and relative proximity to land. Buoy 42007 is just twenty-two nautical miles south of Biloxi, MS, while Buoy 42040 is 64 nautical miles south of Dauphin Island, AL. These two buoys are in the scope of the satellite imagery range and are in relation to the airborne hyperspectral data.

## 2. Current Data

Surface current imagery was gathered as well from <http://oceancurrents.rsmas.miami.edu/atlantic/florida.html> to determine if the surface currents play a significant role on the sediment transport in the region as well. This data was analyzed and placed into seasonal images. These images will be discussed and shown in the Results section of this thesis. These data sets are averaged values over quarterly time frames similar to the method used in determining total absorption. Daily current speeds are

taken and averaged. They are then imaged as arrows, which show direction and speed of the currents.

## **IV. PROCEDURES**

### **A. AIRBORNE HYPERSPECTRAL DATA COLLECTION, PROCESSING, AND SCREENING**

#### **1. Collection**

Airborne hyperspectral imagery was collected with CASI programmed in the spatial mode. This ensured continuous coverage and provided enough spectral range for analysis. The data was also collected on days favorable to instrument operation. Original intent of the data collection by USACE was to survey damage to the barrier islands of Mississippi. Even though the imagery was primarily taken for damage assessment, the number of bands and continuous coverage offered by the spatial mode allows the water surrounding the islands to be examined and limited comparisons to satellite measurements.

#### **2. Processing**

Imagery collected was initially sent to NRL in Washington D.C. for level 1, 2 and 3 processing. Imagery sets were then sent back to USACE in Kiln, MS and analyzed using ArcMap®. ArcMap® is an application found in the ArcGis® Desktop application. True color imagery sets were then transferred to NPS via UPS on a DVD.

The six images were in Tagged Image File Format (TIFF) and ERDAS Image file (RRD) formats. TIF is a true color image which can be processed by most imaging software. RRD is an ERDAS® file format requiring software such as ArcMap® to observe. Images ranged in size from approximately 90 megabytes (Mb) to over 370 Mb.

### **3. Screening**

Due to the limited sample size of the hyperspectral imagery, none of the images are discarded from the study. Though there are only 5 total days, and opportunity to compare the daily changing sediment loads is possible between the hyperspectral and multispectral data sets.

## **B. SATELLITE DATA COLLECTION, PROCESSING, AND SCREENING**

### **1. Data Collection**

MODIS data sets were acquired with permission from NRLSSC using Open-source Project for a Network Data Access Protocol (OPenDAP) on a DODS server. DODS servers allow significant amounts of data to be shared through networking using protocols for requesting and transferring of information. Scientific communities use them for sharing results in experiments while military organizations use them to share other forms of information and data. These servers are secure in that the server host must grant permission to users to gather the data retained on the server. Many programming languages such as Matlab© have commands and functions designed for obtaining information from DODS servers.

Matlab© was used in obtaining MODIS satellite data for analysis from NRLSSC. The two functions loaddap.m and whodap.m found on the website <http://www.opendap.org/> were crucial in obtaining the data. Information gathered from NRLSSC consisted of latitude, longitude, and total absorption in the 488nm, 531nm and 551nm wavelength ranges. The Total Absorption values are based upon the Arnone equations (Lee et. al. 2002) shown in equations (5)-(10).

The total absorption measurements are in units of  $m^{-1}$ , which is a form of voltage. Initially, all values were negative when gathered. Units and values of this nature are uninformative and confusing. Several fairly easy manipulations were completed to make the data more understandable. For example image values ranged from 5000 to 24999 which Matlab© displays as  $10^4$ , so all total absorption values were multiplied by  $10^{-4}$  to place them on a smaller, easier to read scale.

## **2. Processing**

Once the data was downloaded, composite monthly images were made using equations (6), (7) and (8). Once monthly images were produced for the absorption bands, equation (5) was used to produce images of the sediment levels in the Mississippi Bight region.

Data sets downloaded were formed into monthly structure arrays. Each structure varied in size depending on the number of usable images for a given month. Each array within the structure was made up of matrices that were 300x600 cells in size. Each cell represents one 250mx250m pixel.

To make a comparison to the hyperspectral imagery, individual meridional transects were taken to compare image intensity levels along given Longitude lines. It is important to note that 4 to 6 pixels of the MODIS imagery sets are equivalent to an entire CASI meridional transect. This comparison will aid in quantifying how much more information is provided by the hyperspectral imagery and if it is necessary information for the force commanders.

### 3. Screening

All MODIS data sets had absorption values for land being valued at  $-25000\text{m}^{-1}$ . Land values had to be removed before the images could be produced because land was not of interest to this study and can bias results if left in the algorithm. The removal of land was accomplished using Matlab®. Also, pixels containing significant amounts of cloud cover that cannot be resolved were removed. Hurricanes, such as Katrina, have associated cloud coverage that can cover several hundred miles. This tends to limit data that a satellite sensor can acquire. This is apparent in the month of August where only 44 imagery sets were used and five days of data were not processed. Figure (7) shows a 3D pseudo-color image of information gathered for the months of January through April 2005. High pixel sample densities are shown in red while low pixel sample densities are shown in blue. Note that all pixels containing land have been removed and have a density of zero. These images help ascertain locations where the information is limited and should be ignored. For example, in the January figure, pixel density along the  $28.5^{\circ}$  N latitude line is limited and results take this into consideration in that region. February has a region with lower pixel density along the 30th parallel. Results in this region may be partially skewed. March and April both have low spots as well but the sample sizes were much larger. The lighter blue areas still have greater than 10 samples in them. More data density means results are more viable statistically.

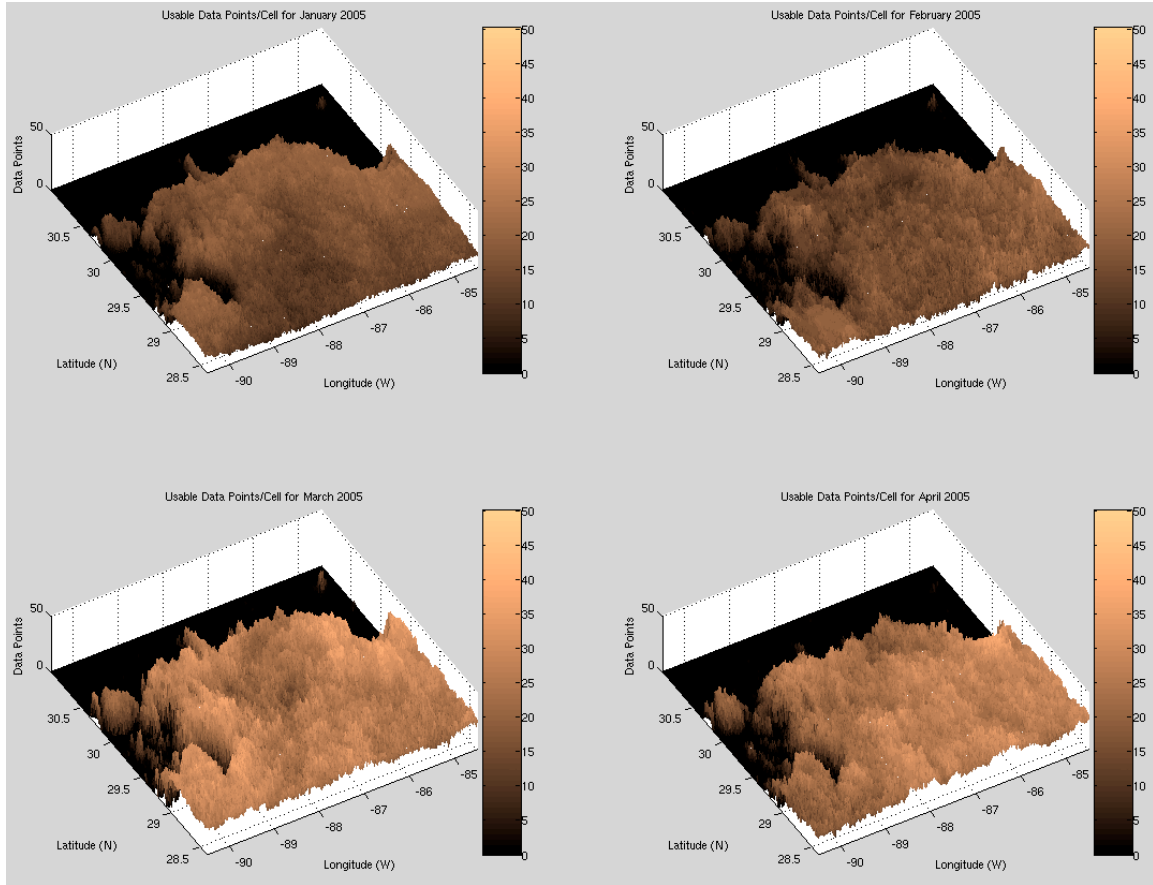


Figure 7. Usable data per pixel for January 2005 to April 2005.

Usable MODIS data for the time frame of August through November 2005 is shown in Figure (8). Notice in August that even though forty-four images were taken, pixel density does not exceed twenty-five. There is also a large spot in the middle with fewer data points. This small data set from August is followed by very large data sets for September, October, and November 2005. This is important when analyzing the affects that a devastating hurricane can have on a particular region.

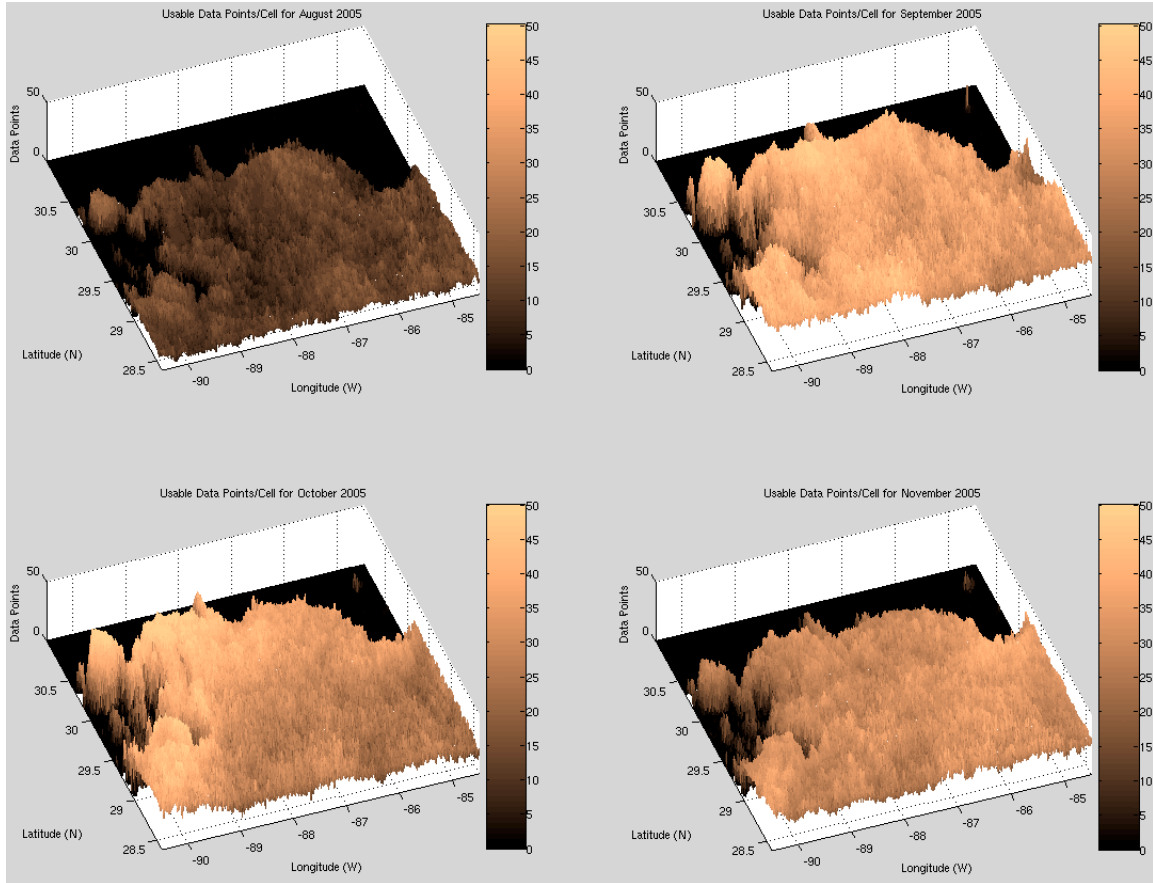


Figure 8. Usable data per pixel for August 2005 through November 2005.

The 2006 Usable pixel data set is shown below. It is important to note that January and February have much larger pixel densities than March and April. This is because of the server failure mentioned previously. March though small, is fairly uniform in its spatial sampling. April however is severely limited on information on the western half of the image. Further analysis will take this small size into consideration.



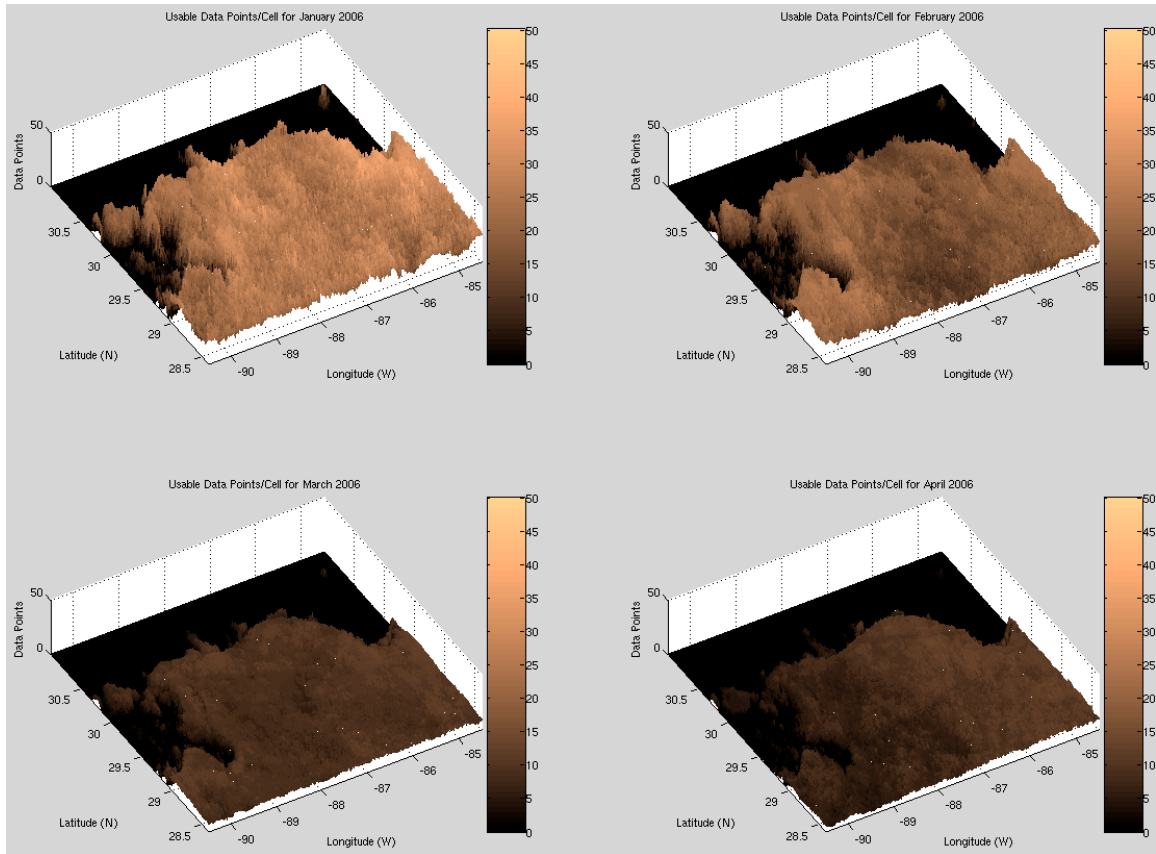


Figure 9. Usable data per pixel for January 2006 through April 2006.

### C. STATISTICAL ANALYSIS

Time series analysis is a technique designed in data sets to determine if measurements follow a non-random order over a certain period of time. Sediment concentrations though highly variable on a daily basis may follow a pattern of high periods of sediment outflow during a given season and lower levels in another season. Using time series analysis it may be possible to anticipate future values of given parameters. This is possible even if the cause of an event is not always identified. Major storm events such as hurricanes may also cause changes that may appear random on a daily scale but might progress with a common pattern over time.

This thesis will look at data sets to determine if there is a seasonal change to the sediment flow in the Mississippi Bight region.

### **1. MODIS Statistical Analysis**

Seasonal or monthly variations in suspended particulate matter concentrations may provide significant information in relation to planning for events in which mine warfare assets are required. Analysis of historical MODIS data may provide insight to future conditions and allow baseline analysis for future operations.

MODIS data is placed into monthly bins and easily accessed this way. A small portion of the earth's surface is not covered by Terra and Aqua because of camera angle changes designed to reduce sun glint. The locations that are not covered vary slightly everyday so that overall coverage of the earth occurs in a given period of time. Therefore, some images of a monthly data set are incomplete. Averaging the daily fields to the fields fills in the gaps and provides a more complete image. Monthly sample means are computed using the following equation:

$$\bar{X} = \frac{\sum_{i=1}^n X_i^2}{n} \quad (12)$$

where  $\bar{X}$  is the sample mean,  $X_i$  is the daily value and  $n$  is the total number of samples. This slight difference in mean calculation is done to convert all negative values in the sample to positive values that are easier to interpret.

Another useful statistic is the amount of daily change that occurs on a monthly basis for the region. Computing the sample standard deviation of the data shown below:

$$s = \sqrt{s^2} \quad (13)$$

is a proven method for determining the change. Here  $s$  is the sample standard deviation and  $s^2$  is the sample variance, which is computed below.

$$s^2 = \sqrt{\frac{\sum_{i=1}^n (X_i^2 - \bar{X}^2)^2}{n-1}} \quad (14)$$

Daily data sets were averaged over a monthly to determine the mean sediment flow. Having a mean flow rate provides the force commander and subordinates with an approximation of the environmental conditions and provides a baseline for making predictions about sensor settings. This allows an operator to fine tune a sensor in the field minimizing the preparation time required prior to entering a minefield. This also reduces the overall time required to clear a mined region.

To explain the statistical analysis, Figure (4) is provided below. This image shows a daily, pseudo-color image of absorption in January 2005 followed by a monthly absorption image. Without bathymetry contours showing location of land the daily image would be unrecognizable. However, the monthly average shows land and ocean clearly. The daily absorption values are slightly higher for the daily sample but not excessively.

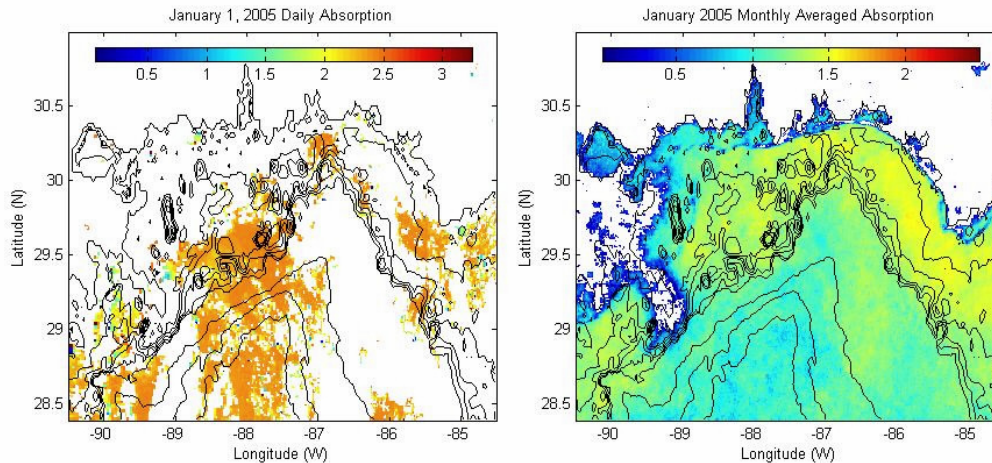


Figure 10. Daily versus monthly averaged absorption values for MODIS.

## 2. CASI Statistical Analysis

CASI hyperspectral data could not be analyzed statistically using time series analysis like the MODIS data was for a simple reason. The sample sizes were too small. Airborne data sets are limited in flight time, area coverage and ultimately cost. Since airborne data sets have a much more limited area coverage, trade-offs must be made between sample repetition and area coverage. The data set reviewed in this analysis covered a larger area to compare sediment flux resolution. The U.S. Army Corps of Engineers also took these data sets. Their goal was to determine the extent of damage done to islands in the region as an aid to gauge how much work would need to be done to repair homes, roads, and other structures in and around the Mississippi barrier island region.

### D. DATA COMPARISON

These two types of data are being analyzed to determine the capability of aiding in the detection of underwater objects such as mines. This includes detection in coastal regions and off shore.

Particle composition is relatively constant below 100m (Twardowski et. al., 2001), but can vary significantly in shallower water. Both sensors are limited to shallow water sensing due to properties inherent to light and water. CASI and MODIS are able to detect sediment in shallower water. How much more information is provided by the hyperspectral imager?

The extent of information can be compared by looking at absorption values along a line of longitude (meridional slice) to determine whether or not the hyperspectral imagery provides amplifying information to the multispectral imagery produced by the satellite.

THIS PAGE INTENTIONALLY LEFT BLANK

## V. RESULTS

Remote, large area coverage, sensors have proven the capability to replace limited coverage, in-situ devices. It is important to apply the proper remote sensor to gather information as all remote sensors do not function equally. In the realm of remote sensing there is a trade off between resolution and area coverage. Monetary constraints may also play a role in sensor usage and deployment tactics. Airborne sensors such as CASI are fairly cheap when initially purchased but future costs may be high due to airplane maintenance, fuel costs etc. Satellites have a very high initial cost but after launch require very little to maintain. In either case it is important that the sensor collect the data needed to aid the forces preparing to fight.

The following image provides an overview of all of the data analysis that was completed and where samples were taken from. The black barbed lines are locations where monthly cross sectional data sets analysis was completed. The first meridional cross section also falls in the one location where hyperspectral imagery has a continuous set of intensity values allowing the hyperspectral data to be compared to the multispectral data. A zonal cross section was taken also to observe whether or not there are differences between the meridional and zonal absorption values.

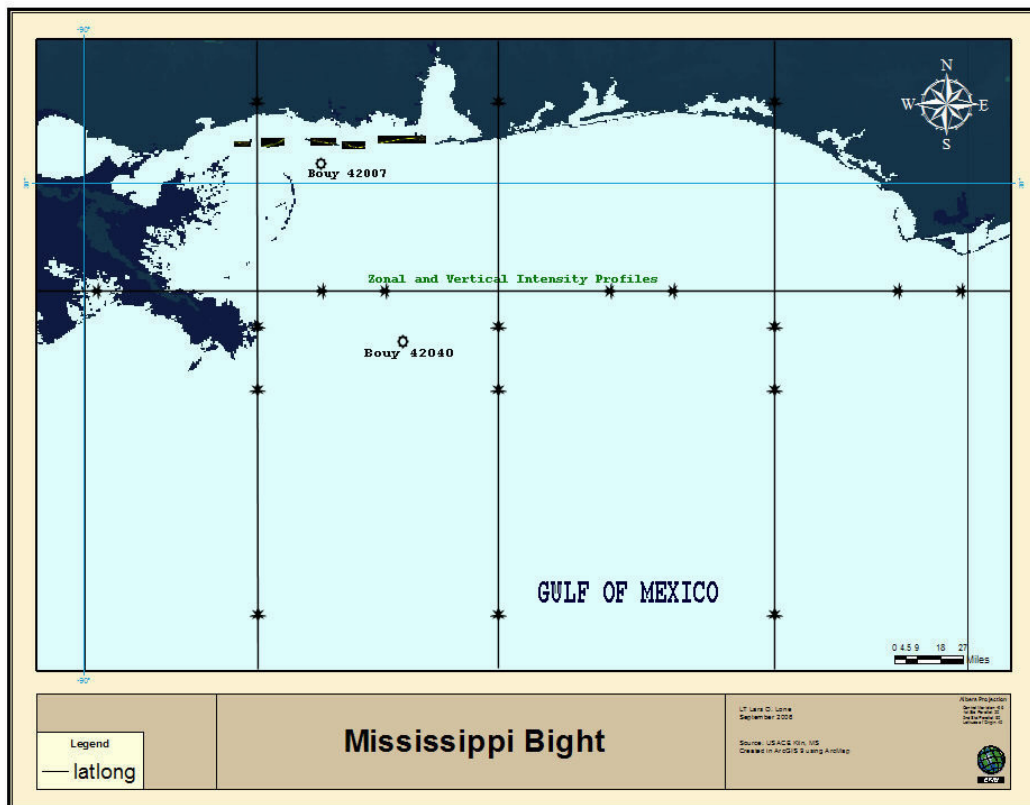


Figure 11. Data evaluation overview showing locations of data set analysis.

#### A. HYPERSPECTRAL IMAGERY ANALYSIS

Airborne hyperspectral imagery is increasingly valuable at the tactical level. It is small enough to be attached to a UAV and can return very detailed images of an area in question. Much can be determined from shipping channels to sand bars. Many moored mines are greater than one meter in diameter as well, meaning that this sort of imagery could be used to detect and possibly classify mines and locate obstructions that may be in a channel or on a beach of interest to the operational forces. Figures (12) and (13) show the difference between CASI airborne true color imagery and that of MODIS satellite true color imagery. The hyperspectral image of Dauphin Island shows



sediment plumes, shipping channels, and sand bars. This information is just not possible to obtain with satellite imagery. This is evident in Figure (13), as Dauphin Island appears as a white line along the 88th parallel. No island features can be seen by satellite, nor the small inlets or shipping channels.



Figure 12. CASI True color hyperspectral image of the east side of Dauphin Island (1 m resolution).



Figure 13. MODIS true color multispectral image of all Mississippi Barrier Islands (250 m resolution)  
<http://www7333.nrlssc.navy.mil/>

Notice in the image of Dauphin Island that the boat channel in the upper middle part of the picture can be seen as well as sediment depositions on either side of the channel. Closer inspection also reveals suspended sediment plumes in many locations. Dauphin Island also does not appear to be damaged too severely, however this is not the case in all of the barrier islands. Cat Island for example, which is directly south of Gulfport, Mississippi, was directly in line with Hurricane Katrina. Prior to the storm Cat Island was covered with vegetation. After Hurricane Katrina, it was barren. This is important information for force commanders because all of the vegetation was forced into the ocean producing obstacles for shipping. Floating trees can cause significant damage to a wooden-hull vessel such as a minesweeper. An image below shows the devastation done to Cat Island.

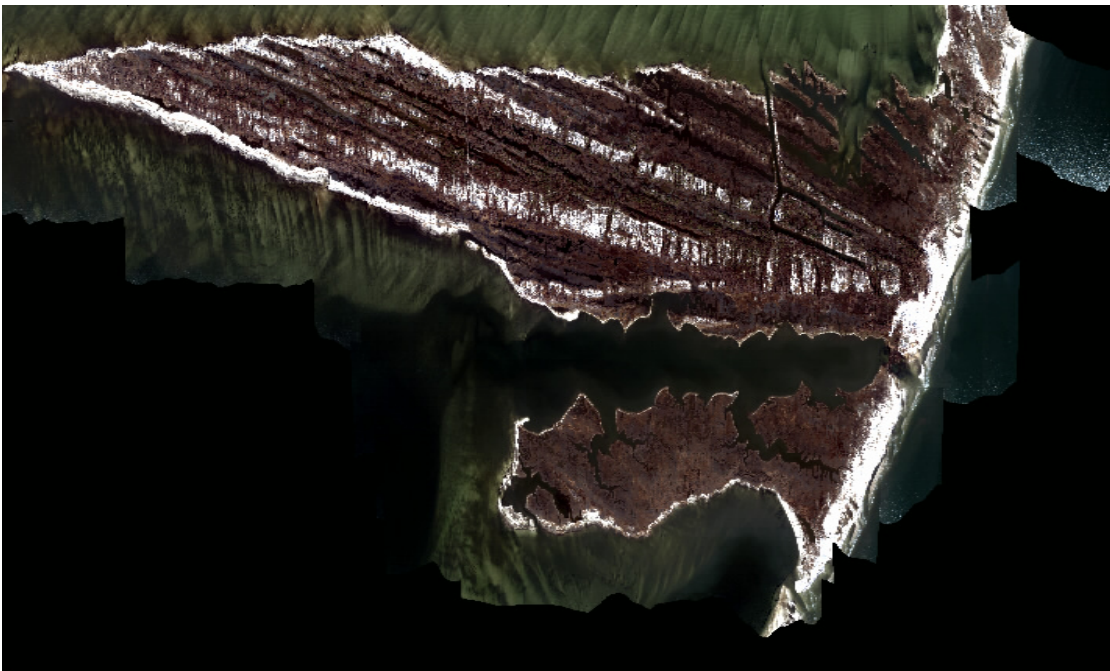


Figure 14. Cat Island after Hurricane Katrina. Image taken by CASI November 29, 2005.

CAT Island has very shallow water on the west side of the island but notice the color change on the east side. This darker blue water shows that the water is significantly deeper on that side of the island. It is also lacking sediment depositions meaning it would be much easier to hunt and clear mines on this side of the island.

## **B. MULTISPECTRAL IMAGERY ANALYSIS**

### **1. Yearly Multispectral Comparisons**

Comparisons of satellite imagery were completed to determine the overall change in absorption. Bathymetry contours were added to see if depth was a factor in how much total light was present. Contours are shown at 0,20,40,60,80,100,500,1000, and 1500m increments for each of the images. It is apparent that in several months such as January (and somewhat in March), that the ocean's bathymetry does have an affect on the amount of absorption or reflectance. Higher reflectance values track along the 100m-depth contour line. A significant change is seen in April 2005 (the bottom right image). This could be due to a change in wind patterns and surface currents. These two factors are explored further on in this chapter.

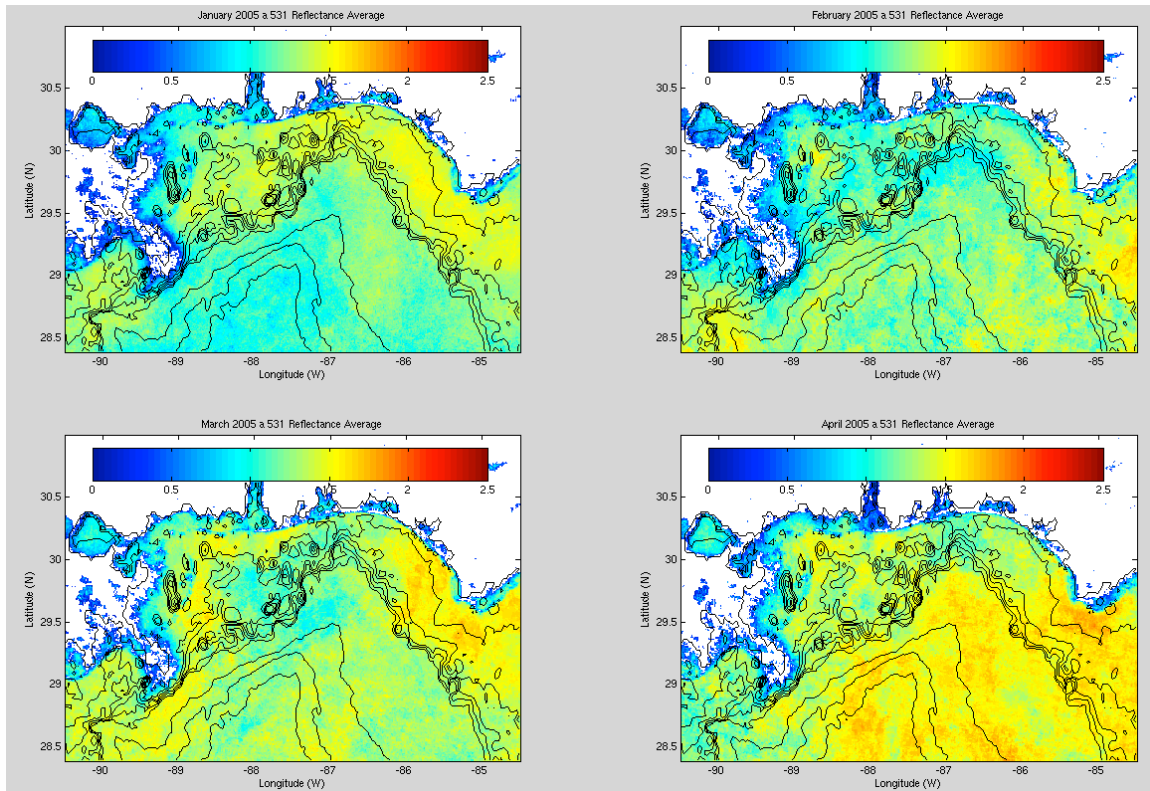


Figure 15. January to April 2005 monthly reflectance averages.

The four images above are compared to those of 2006 to see if the reflectance averages changed due to the excessive stormy season seen in the later part of 2005. Reflectance values in 2006 are much higher than those of 2005 with the most extreme case occurring in March 2006. February 2005 (top right) appears to follow the 100m-depth contour fairly well but the other three images do not. March 2006 (bottom left) extremely high values may be caused by the relatively small sample size, which was mentioned in the previous chapter but may be validated by results shown in the following month of April. Note that in April 2006, the highest reflectance values are seen on the side of the image where the highest density of samples per pixel is taken. The density of samples in March was very uniform giving a high reflectance reading. It is



likely that April experienced similar high values all over but this shift may also be caused by a change in currents during this time. The surface currents do shift from heading westerly to a predominant easterly direction during this time frame.

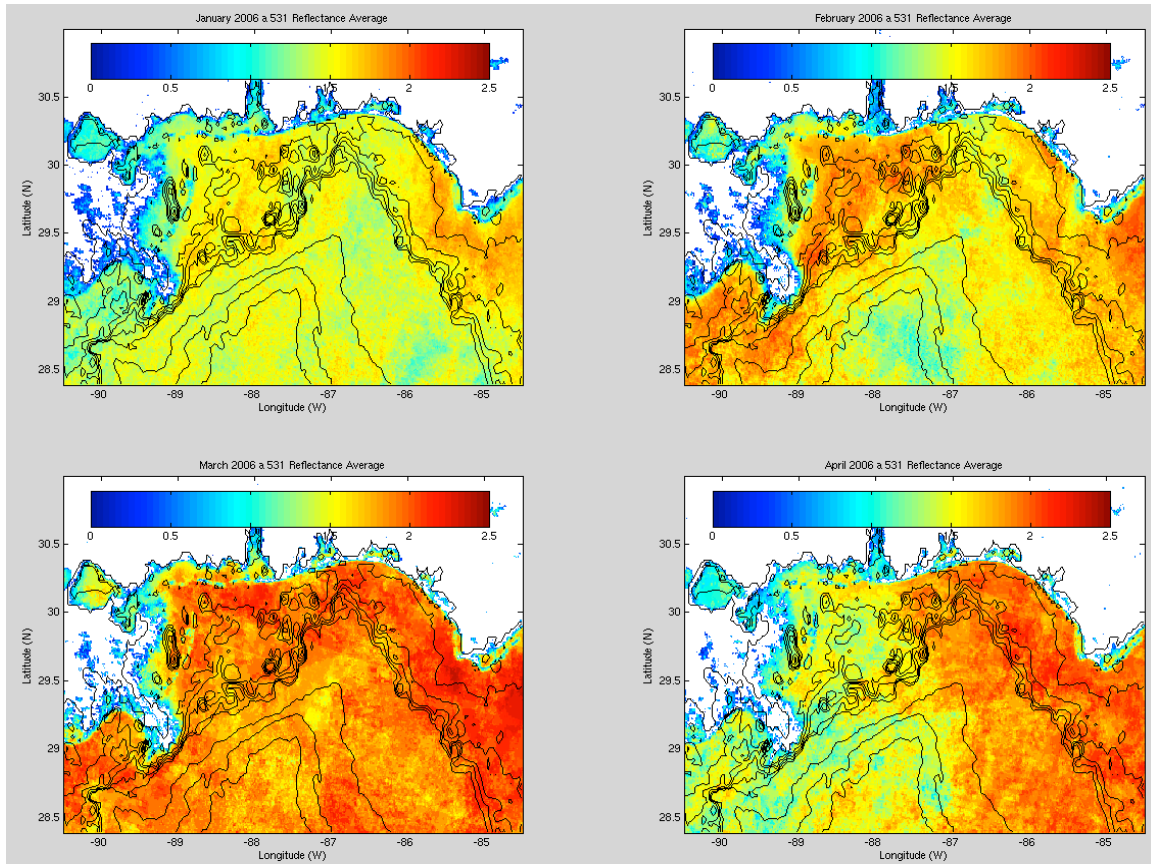


Figure 16. January to April 2006 monthly reflectance averages.

Three meridional transects at  $89.0^{\circ}$  west,  $87.5^{\circ}$  west and  $86.0^{\circ}$  west were completed to further compare differences and see if changes in total absorption and reflectance. The months that were analyzed were the same as noted and shown above.

The left side of each of the following figures represents the northern most point of the satellite data

set collected and is over land, hence no reflectance values. The right side of the figures below is the southern most point of the satellite imagery. At all three longitudinal transects the reflectance values for 2005 are lower than those of 2006, which coincides with the images shown above. Some trends are noticeable along the first and third transects. The significant drop along the  $89.009^{\circ}$  west transect (far left image) at approximately  $29.15^{\circ}$  north Latitude is caused by a crossing of the North Mud Lumps located at the mouth of the Mississippi River. The curve is more drastic in 2006 due to the significant erosion caused by the stormy season. Reflectance is higher further out to sea along the  $87.5^{\circ}$  west (middle figure) longitude line implying that the sediment is being pushed off shore. This mostly offshore transport is most likely caused by wind forcing.

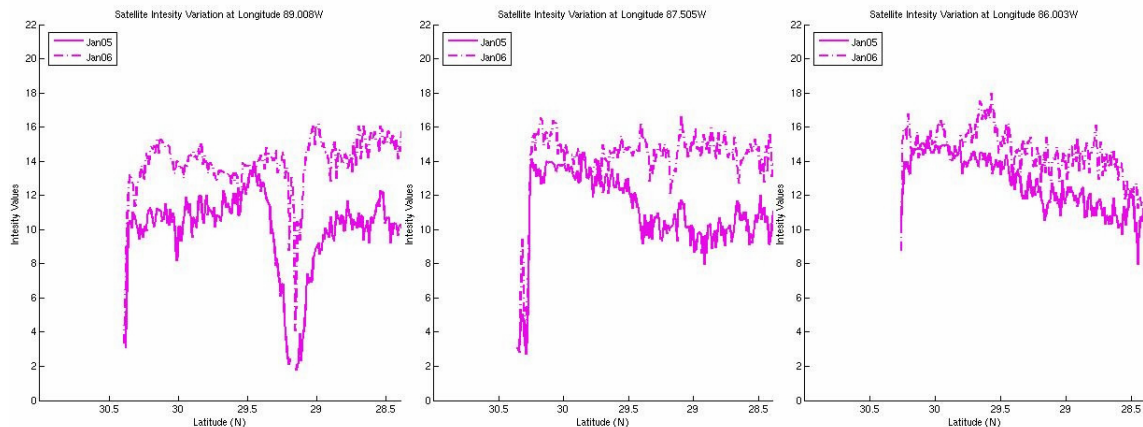


Figure 17. Yearly total absorption for three longitude lines for January months.

Similarities can be seen in February as well. However, a major difference is seen along the  $87.5^{\circ}$  West longitude line. It is opposite of what is seen during the January months and this flip-flop is most likely cause by

increased current activity and a reduction in wind forcing. A drastic change is also seen near the Mississippi North Mud Lumps as well where significantly higher values are seen during the 2006 season. More sediment is suspended in this region than previously seen. Erosion inland and the westerly currents keep the suspended sediments closer to shore are the likely cause of these higher values.

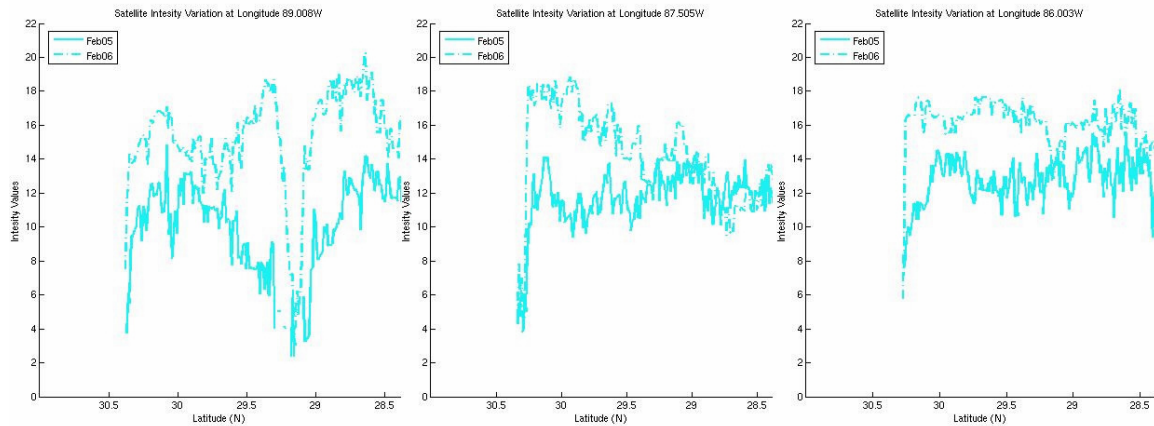


Figure 18. Yearly total absorption for three longitude lines for February months.

Longitudinal transects for March clearly show the changes already noted in figures 15 and 16. As stated before, this is likely caused by the strong winds in the area driving the surface currents, which begin to change during this time as well.

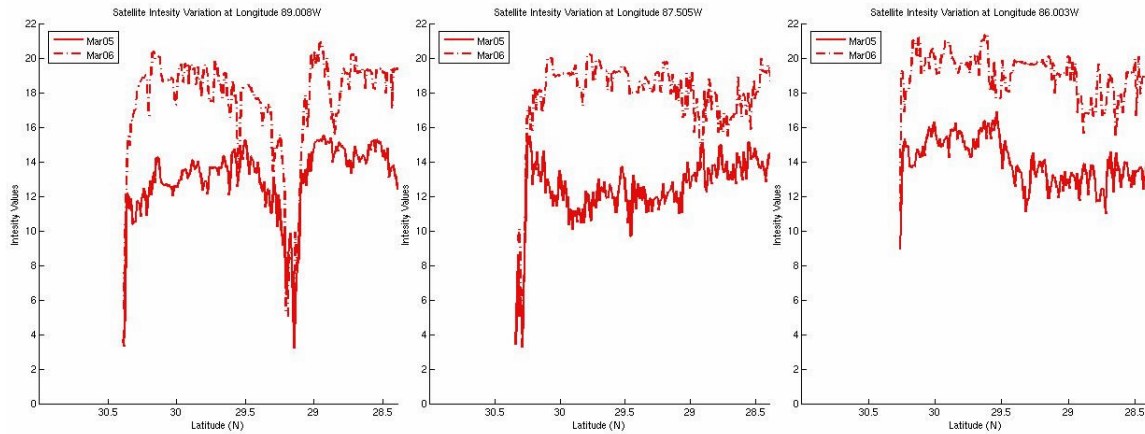


Figure 19. Yearly total absorption for three longitude lines for March months.

April 2005 and 2006 along the 89.0<sup>0</sup> West longitude line are fairly similar. This may be caused by several reasons; data set size during 2006 in this area is low causing inaccurate results for 2006, or a settling of suspended sediments in this area, or a shifting of currents pushing sediments to the east. Any or all three of the possibilities could cause this similarity.

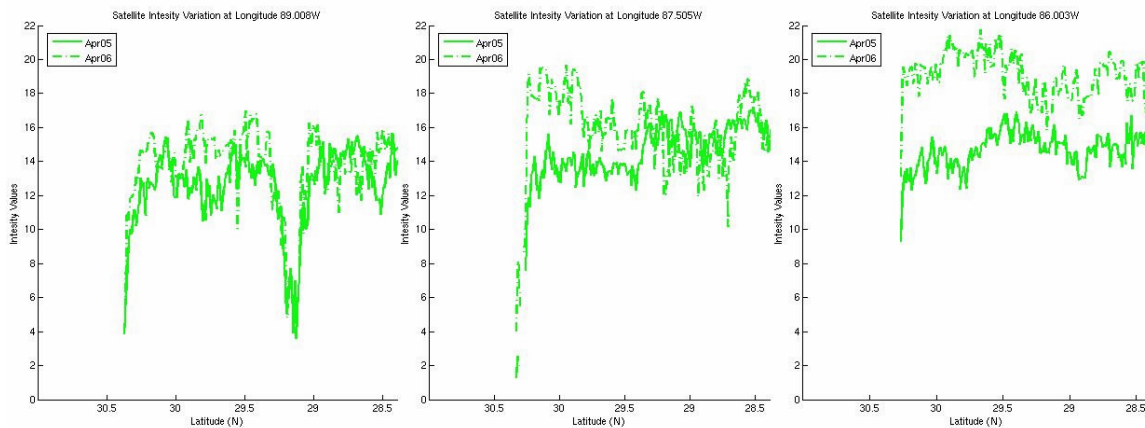


Figure 20. Yearly total absorption for three longitude lines for April months.

There is an overall yearly difference in reflectance. This necessitates gathering data yearly prior to a major



operation to understand how the environment has affected the ocean climate.

## **2. Monthly Multispectral Imagery Comparison**

Monthly multispectral imagery during the hurricane season was also gathered to see how major storms change the reflectance values of the ocean. Like the monthly data above, this set of images span a four month period starting in August and end in November 2005. To better grasp the impact of hurricane Katrina, the days following hurricane Katrina are added to September's data set. Katrina became a Hurricane on the August 24, 2005, and made landfall around the 29th. Four days of information during this time data was not gathered due to storm intensity, power outages, etc. This left only two days of August data added to the September data set and does not affect monthly averages significantly. Shown below, are the four monthly reflectance averages. Reflectance values during August are low, mostly affected by prevailing currents. This will be evident upon reviewing the wind data in figure (25). Significant changes are seen in the following months. Hurricane Rita also passed through the area in late September, which would cause the shifting of sediment to coastal regions as October shows. Wind and surface currents predominant in the region spread the suspended sediment out as is shown in November. Also note the significant flooding present between August and September.

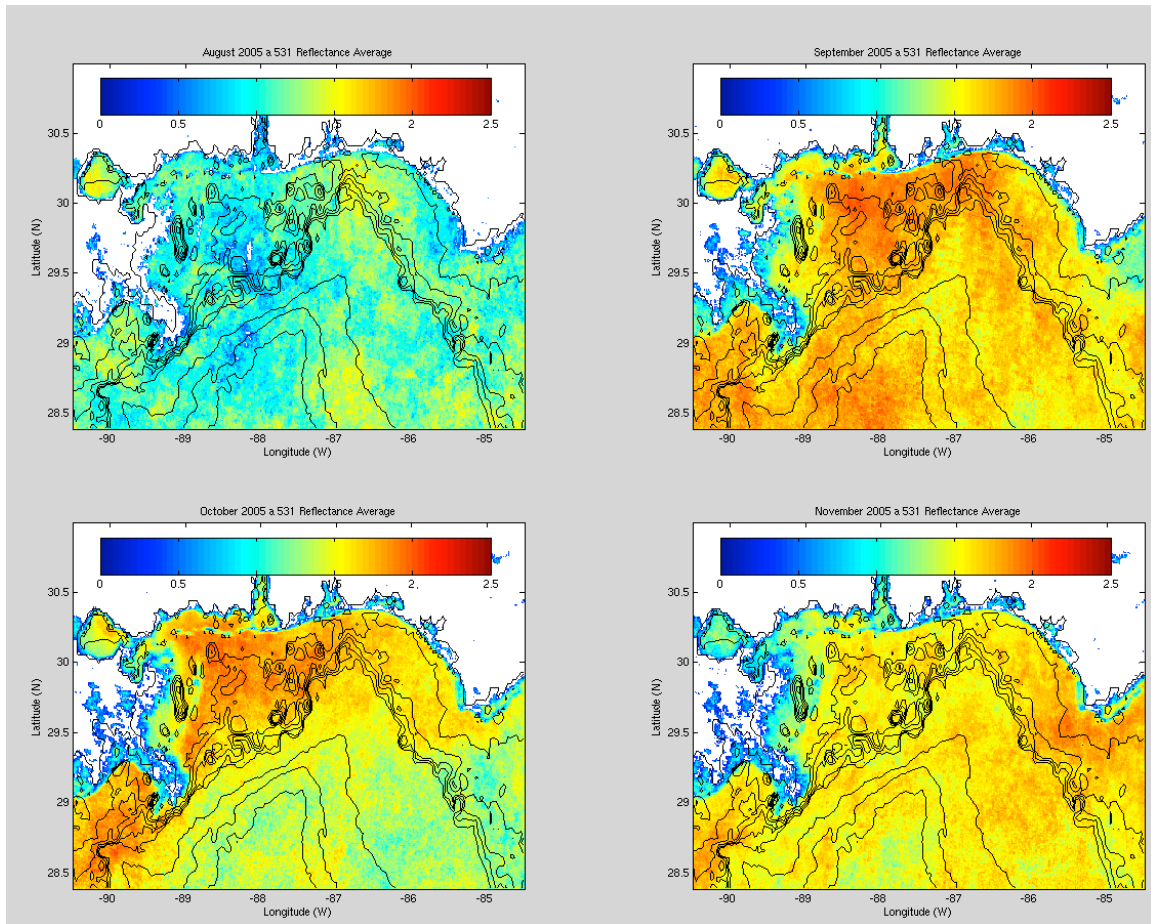


Figure 21. August to November 2006 monthly reflectance averages.

A meridional transect at three points for the four months was also accomplished. The longitude points locations for the monthly comparison is the same as those used in the yearly comparison. Points for February 05 were added as well to show an interannual change February had similar value ranges as August and further show an extreme change that can occur do to large storm events. There is a significant increase in reflectance during September and October along the  $89.0^{\circ}$  West longitude line. November starts out similar to August but nearer the Mississippi North Mud Lumps reflectance increases and stays elevated like September and October most likely because of sediment

expelling from the Mississippi River. The highest values are seen in October at  $89.0^{\circ}$  West and are due to the two hurricanes that passed through the area. This is also the reason value for October resemble August more along the  $86.0^{\circ}$  West transect.

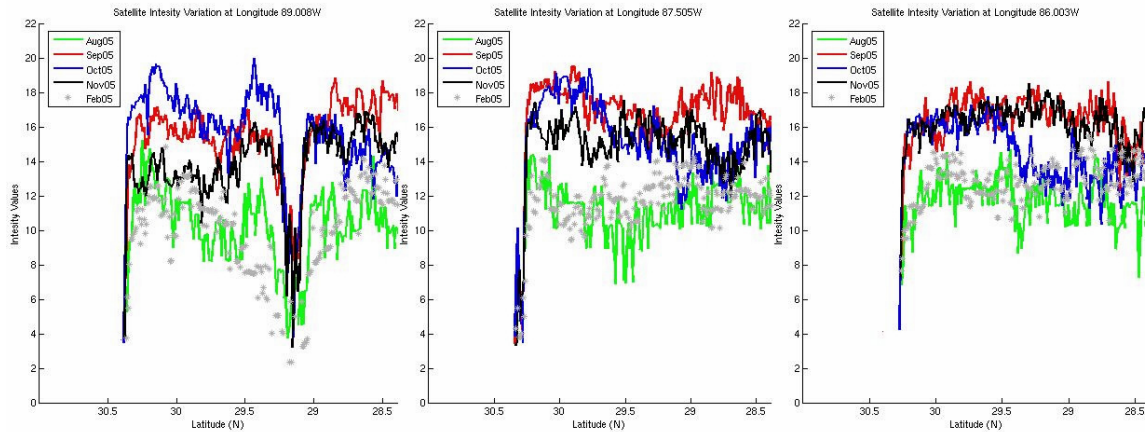


Figure 22. Monthly total absorption for three longitude lines from August to November 2005.

One zonal track along  $29.5^{\circ}$  North Latitude was completed to see if similar results would show lengthwise along the image. The first small set of values near  $90.5^{\circ}$  West is from the bay south and west of the Mississippi River. This zonal transect then crosses land over the Louisiana Peninsula. Notice September and October values approach August values around  $85.0^{\circ}$  West. This was the region least affected by hurricanes Katrina and Rita. It is high here in November because of hurricane Wilma that struck Florida.

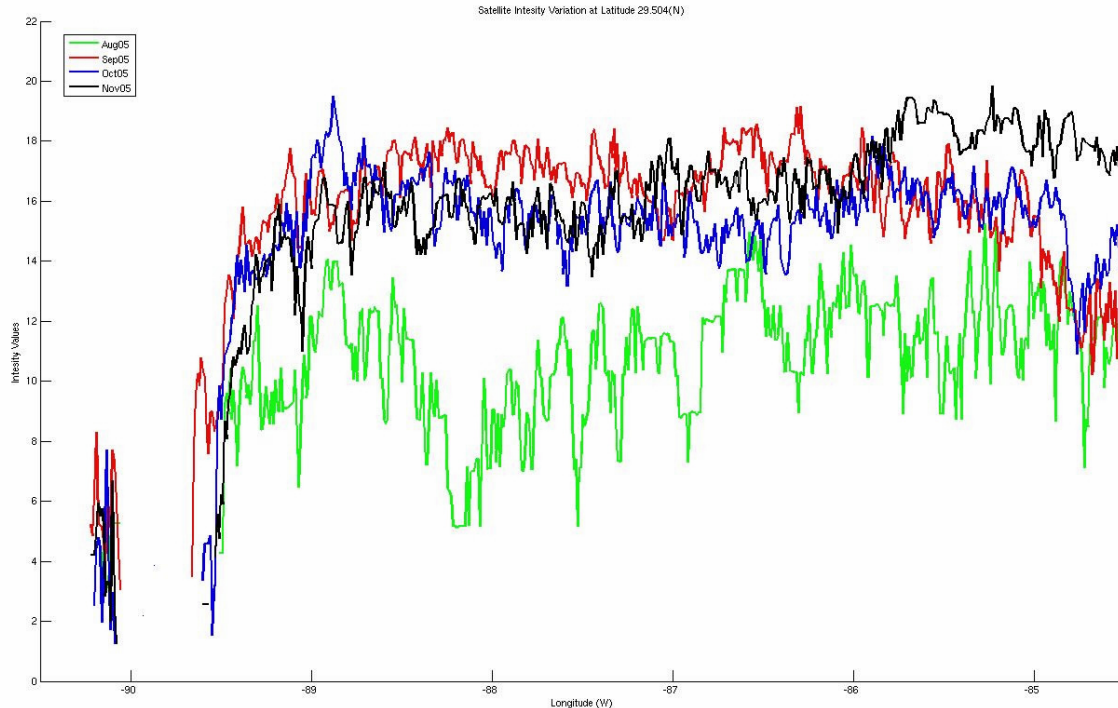


Figure 23. Monthly zonal total absorption from August to November 2005.

### 3. MODIS Suspended Sediment Assessment

Total absorption measurements do not segregate between types of solids in the water. All solids reflect light that can be measured by a sensor. Equation eleven is an equation specifically designed and tested to measure suspended sediment values. Below are a series of images depicting suspended sediment concentrations for January-April, August-November 2005 and January-April 2006.

Suspended sediment concentrations tend to be higher in the west bay of the Mississippi River delta, along the coast during the early season. It is evident in both January and February. Similar concentrations are seen near Florida on the east side of the image as well. March shows a change where large concentrations of suspended sediment move off shore. This sediment is then transferred into the East side of the Mississippi River delta and is most likely

caused by the current changes shown above. Notice also that the sediments track along the contour lines as well.

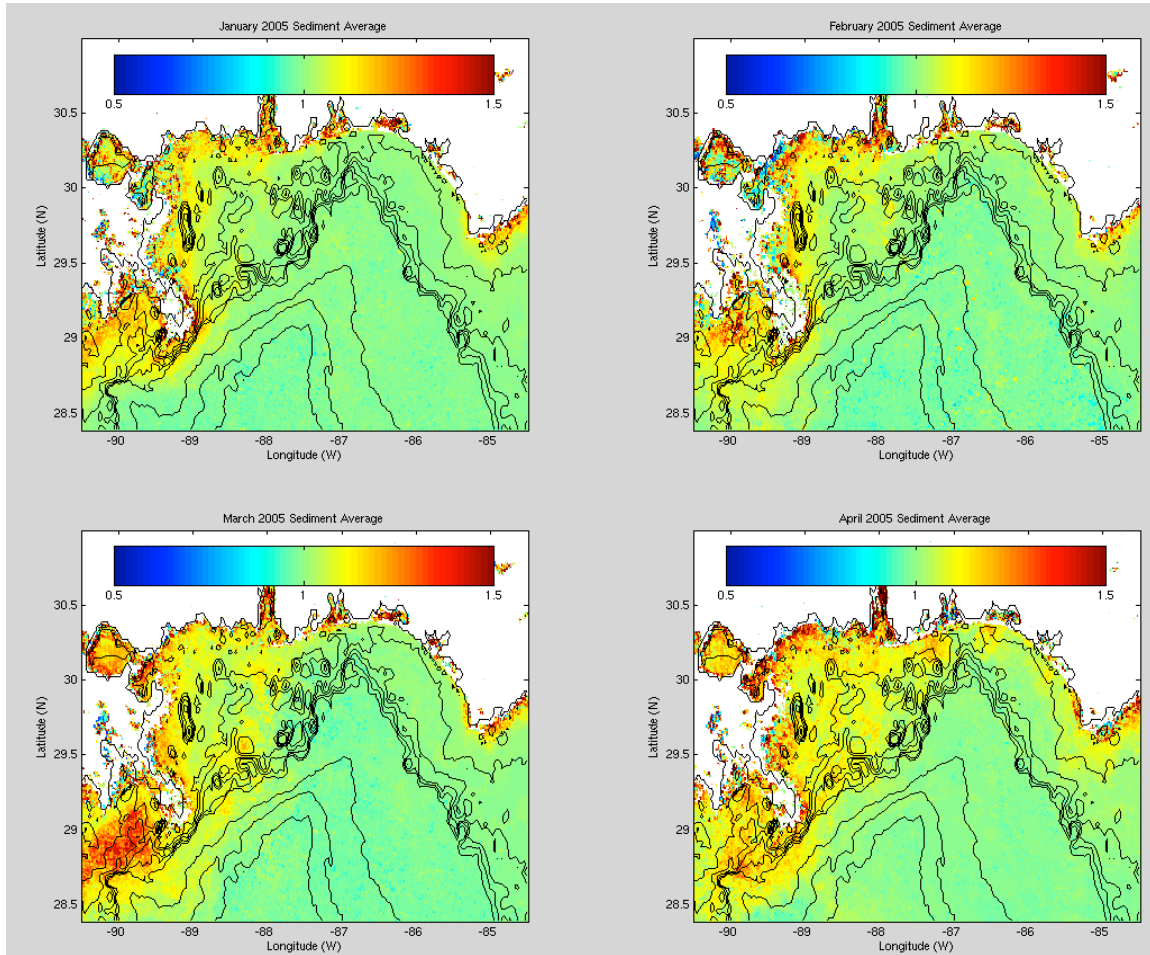


Figure 24. January to April 2005 suspended sediment concentrations in the Mississippi Bight region.

August to November show a major shift in sediment loads as well. Low wind and wave activity tend to keep the sediments close to the shore in shallower water. After hurricane Katrina, large amounts of sediment were transported off shore. This affect is not clearly seen after hurricane Rita in November's plot probably because of the shift in the surface currents and other environmental factors. Also note that sediment concentrations track



along the depth contours fairly well. Especially around the Florida coast ( $85.5^{\circ}$ – $84.5^{\circ}$  W longitude) concentrations build up at contour lines as seen very well in August.

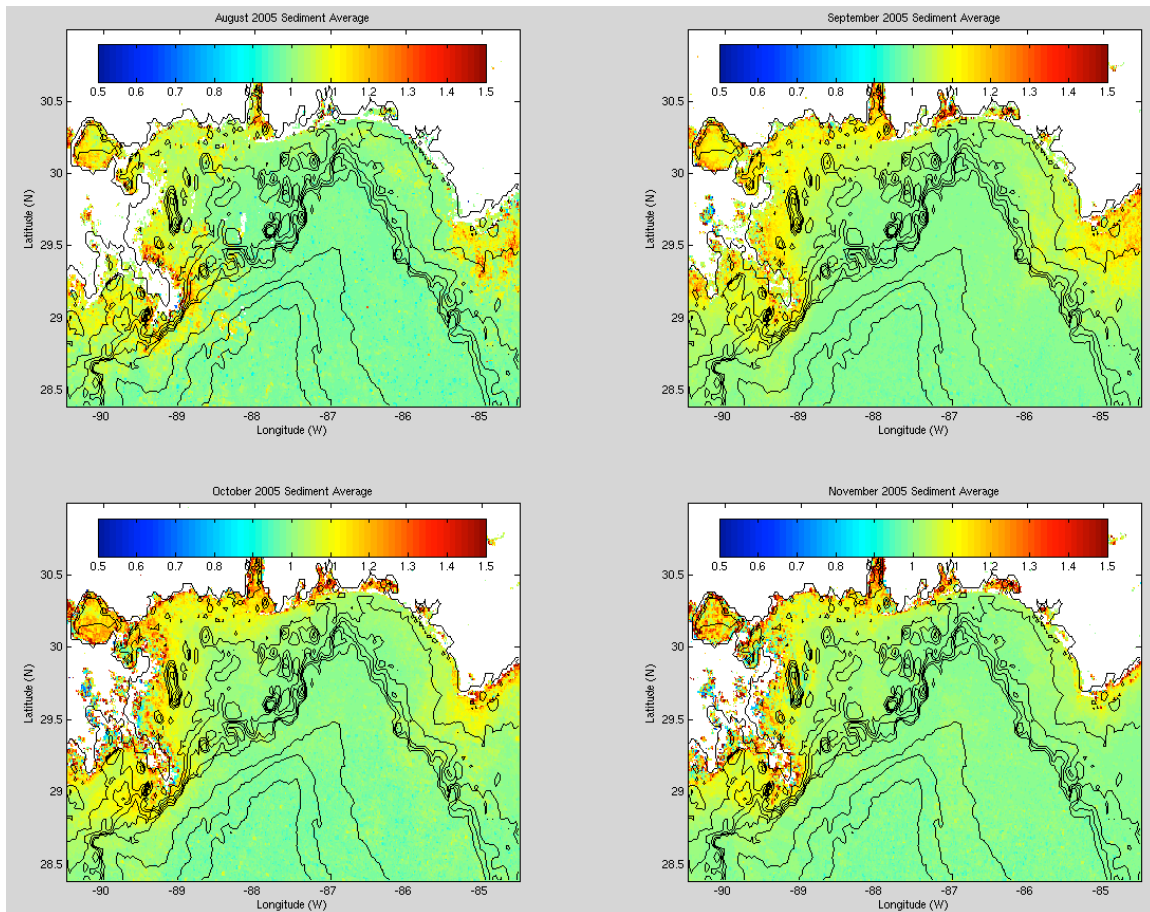


Figure 25. August to November 2005 suspended sediment concentrations in the Mississippi Bight region.

Sediment concentrations can be tracked moving offshore between January 2006 and February 2006. A similar shift occurred in March 2005. This change could be due to the significant wind forcing and storm activity that took place during the month of January. A relaxing of the currents during April 2006 spawns an off shore concentration of sediments in the western bay of the Mississippi River as well.

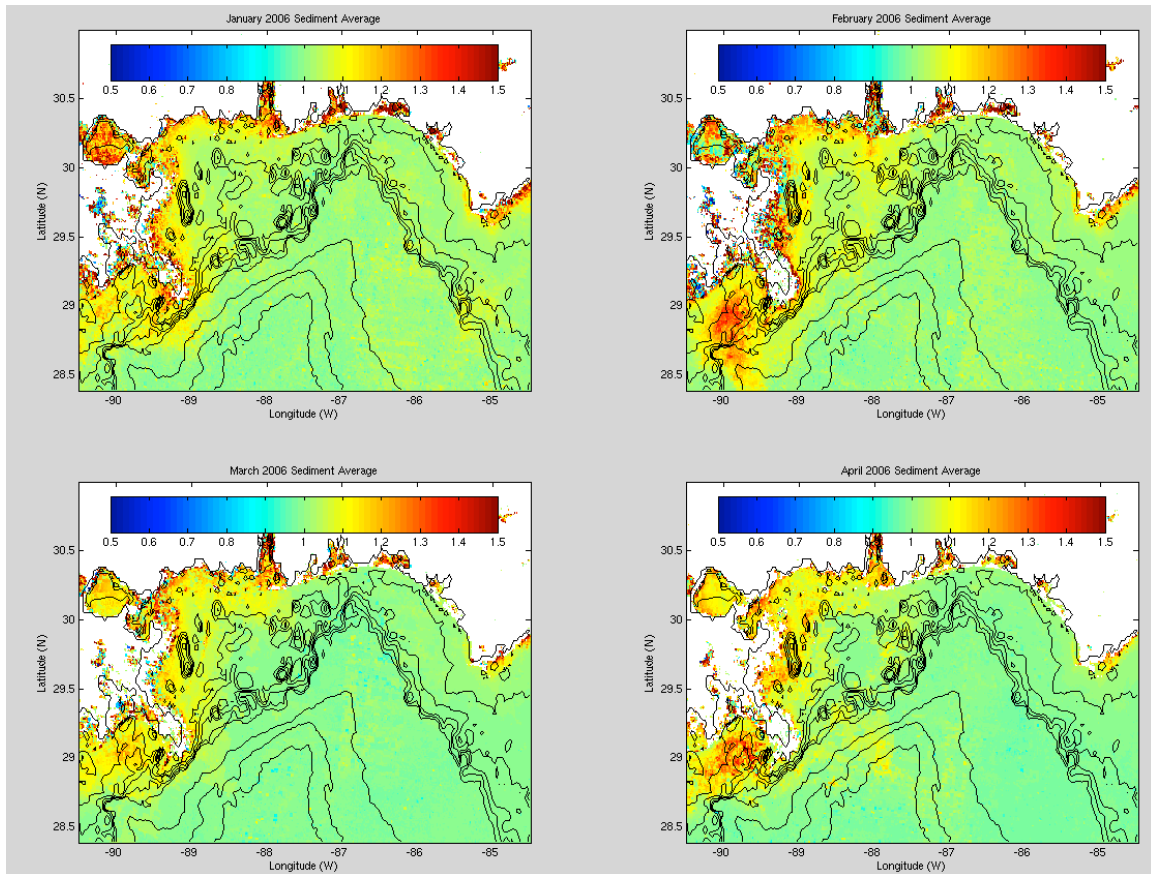


Figure 26. January to April 2006 suspended sediment concentrations in the Mississippi Bight region.

#### 4. Wind and Surface Current Evaluation

As previously mentioned wind data from NDBC from buoys 24007 and 24040 was taken to determine how wind affected a given point in the study area. The following graph is a time series of daily wind speeds beginning January 1, 2005 and ending on April 30, 2006. Months that were not used in the study were grayed out. January 1, 2006 to April 30, 2006 are shown in black and show the difference in the yearly wind values. The higher wind speed peaks during the 2006 year help explain why reflectance in 2006 is higher than 2005. Also notice the very low wind speeds during the month of August. Hurricane Katrina is easily identified at the end of August and hurricane Rita is also evident at the

end of September. Wind speeds at both buoys are very similar so the only time series that will be shown is that for buoy 42040.

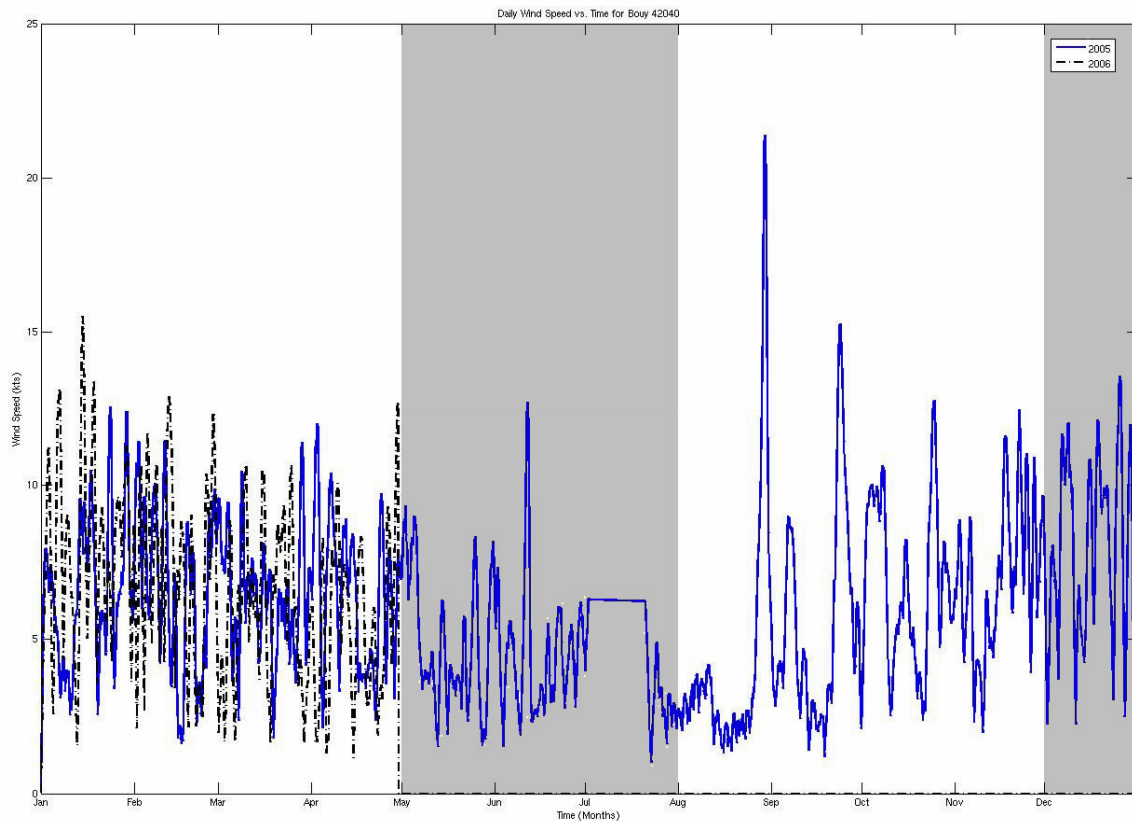


Figure 27. Time series of daily wind speeds for buoy 42040.

An average wind speed per month is computed and graphed against reflectance averages and is shown below. Notice that wind values are very similar at most points. The only noticeable differences in off shore and on shore wind speeds come in January and February 2006 where off shore speeds are slightly higher. Some months like October 2005 have the same wind speed but very different reflectance values at the two points. This implies that other affects are altering the reflectance values. A very likely cause for the difference comes from the surface



currents. Buoy 42007 has reflectance values higher than those of buoy 42040 which makes sense also because it is closer to the Mississippi River and in shallower water where waves are more likely to interact with the ocean floor and entrain sediments.

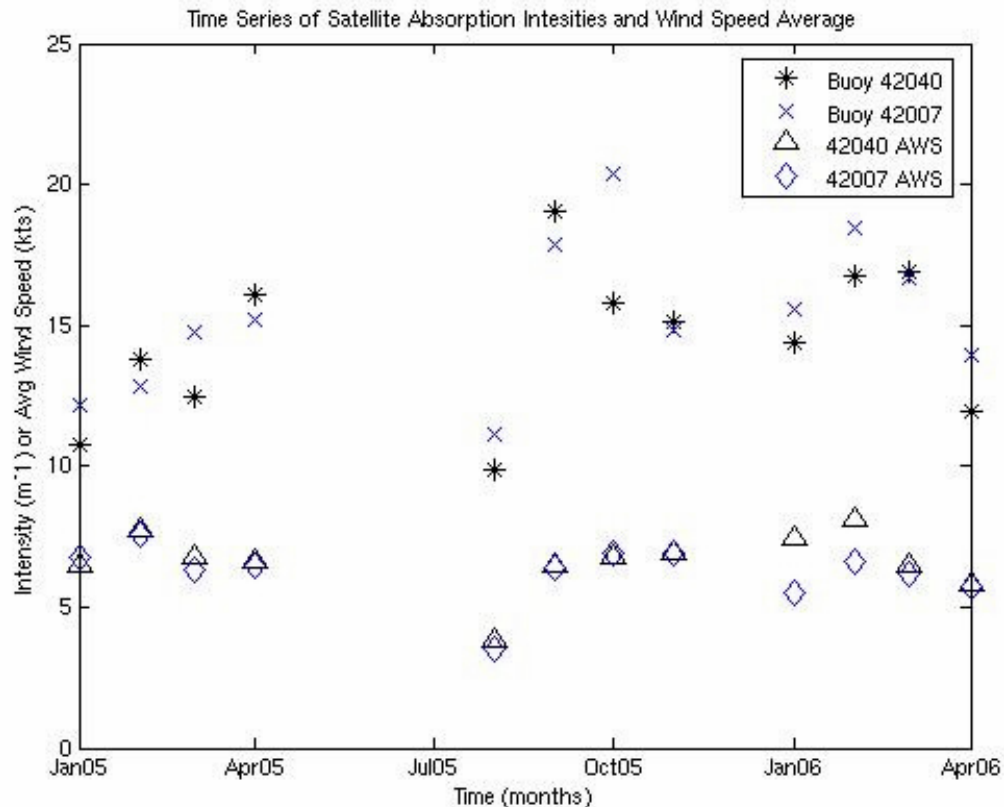


Figure 28. Single point time series comparison of monthly total absorption to wind speed.

The following images depict how surface currents change over the course of a year. These images are averaged for each quarter. Notice in the first quarter, a large variability in direction around the Mississippi Gulf Coast region. Quarter two reveals a significant shift in ocean currents in the gulf. The currents are more aligned in an easterly direction. This would explain why

reflectance values on the eastern side of April 2006 are higher than those found on the west side of the image. Temperatures for the region are also shown. The Gulf warms during the second quarter. This temperature change could cause reflectance differences as well.

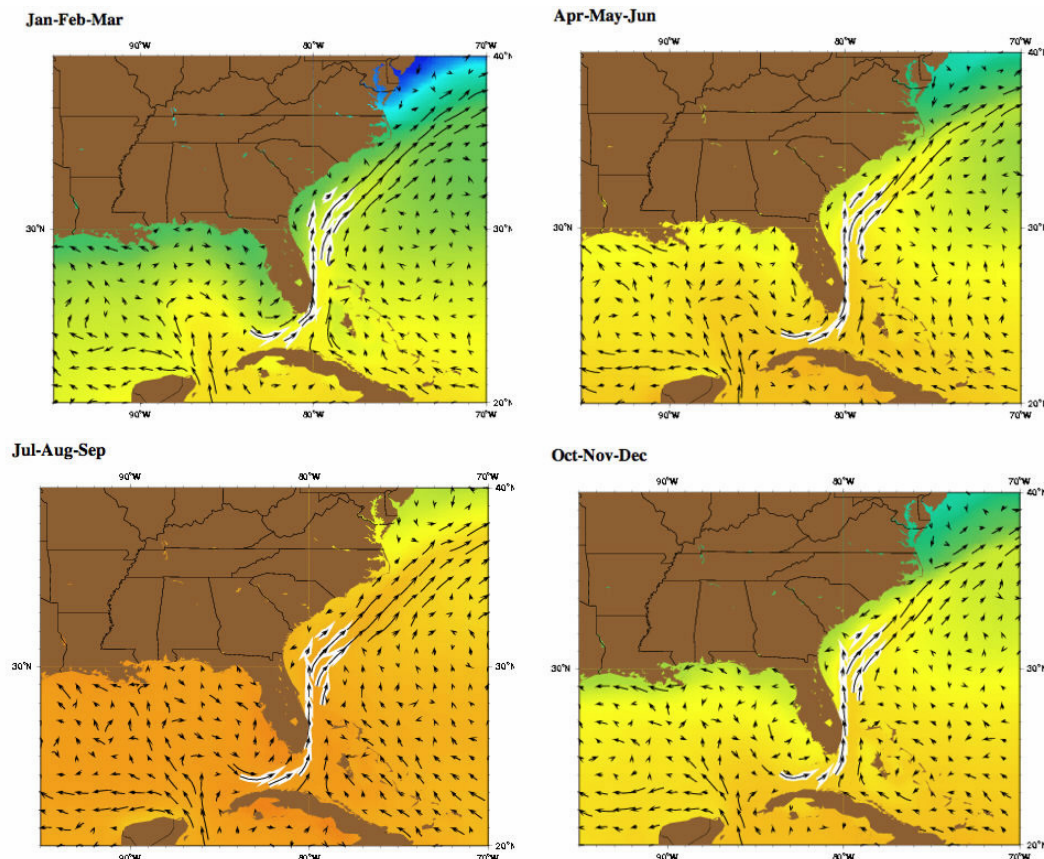


Figure 29. Four quarter surface current averages.  
<http://oceancurrents.rsmas.miami.edu/>

### C. AIRBORNE VS. SATELLITE COMPARISON

As shown above in the images of Dauphin Island and Cat Island, all of the images are primarily composed of landmasses. When absorption values for land are removed from the images, there are typically around 100m in length of data remaining in any given direction, which is less than the 250m-pixel resolution of the satellite imagery.

The only image containing a continuous patch of water for a distance greater than 250m was that of Ship Island taken October 30, 2005. A meridional slice of absorption values was taken of the water west of Ship Island and intensity values were compared to those of October's intensity values. Both data sets were normalized so that values would be on the same scale. This meridional slice was taken at approximately  $89.0^{\circ}$  West Longitude. It is readily apparent that hyperspectral imagery gathered at low altitude by an airplane can gather significantly more information than that of a satellite. Notice also that both have a low point near  $30.212^{\circ}$  N latitude, and there is an upward trend in both sets after  $20.21^{\circ}$  N latitude. This implies that even though the satellite data does not have the variability it is still useful data.

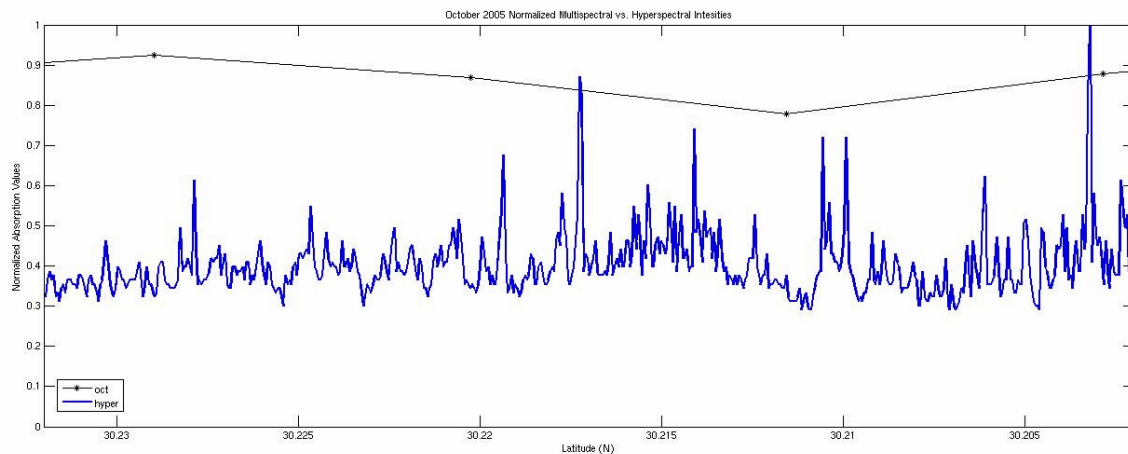


Figure 30. October 2005 comparison of normalized absorption values of a meridional transect of satellite multispectral imagery and airborne hyperspectral imagery.

THIS PAGE INTENTIONALLY LEFT BLANK

## **VI. CONCLUSIONS AND RECOMMENDATIONS**

### **A. CONCLUSIONS**

CASI has proven to be a very useful imager. Its high-resolution capability is good enough to detect very small-scale suspended sediment events. CASI might also possess the ability to detect moored mines due to their size and possibly some bottom mines in shallow water. This detection could aid in maneuvering a battle force to a region where there are no mines allowing for more rapid deployment of troops.

CASI is also very versatile, capable of operating in several modes depending upon the needs. With a battlefield that is constantly changing and an environment that is just as unpredictable, it is important to have sensors that can be modified for the situation. Hyperspectral imagers that provide multiple modes would support field operations greatly.

Portability of the hyperspectral imager is also useful. Its capability to be mounted on several different types of aircraft further extends the versatility of sensor. Any ship with the capability to launch and recover an aircraft or helicopter could potentially have one of these sensors on board prepared to deploy at any time.

Airborne hyperspectral imagers do have some drawbacks. Limited coverage of an area means primary usage would be at the tactical level. Since they are deployed onboard an airplane, they are overt. This limits the amount of surveillance that can be done. It also gives an enemy an idea of where battle forces want to attack, thereby reducing the element of surprise.

Another drawback is file size. Currently collected data set cannot be analyzed on the aircraft. It must be brought back and analyzed separately. The data set in this study took over a month to acquire. This may have been because the data was not time critical for United States Army Corps of Engineers (USACE). If the data were time critical as in a battlefield situation the data would be analyzed in a more timely fashion.

During the 2005 hurricane season, a major storm was seen every month. Planning operations may require the more rapid deployment capability that an airborne sensor provides to determine a safe passage through an area of interest, in order to ensure a force is not delayed by follow-on storm activity.

Satellite multispectral imagery is also very useful to mine warfare. Though it lacks the high resolution of airborne sensors it has several useful qualities. First of its qualities is covertness. Regions of interest can be seen almost daily by MODIS without giving the enemy ideas of current intent. This aids in planning and battle preparation. MODIS also provides large-scale coverage of a region, which is impractical to use an airborne sensor to do.

Data sets also point to the possibility of anticipating sediment loads in a given region especially during the calm season. Understanding the sediment load in a particular region allows fine-tuning of the underwater sensors. This aids in both rapid detection of mines and extended range of detection.

January, February, March, and April data sets in 2005 and 2006 showed monthly variations both near shore and off shore revealing the necessity to continuously survey a region of interest. The smaller data sets of 2006 still provided significant amounts of information just the larger data sets of 2005 did. August through November 2005 showed many suspended sediment changes due to the major storm fronts. These storms play a major role in how the sediments are distributed.

## **B. RECOMMENDATIONS**

Continued testing of the CASI instrument is necessary to determine fully its capability and the contribution it can provide to the war fighter. It is hard to determine sediment flow with an image that is primarily made up of land as well. Future imagery of just the water column might provide much more information about the suspended sediment transport.

MODIS products have been and should continue being used to provide the war fighter and force commanders with battle space information. Satellite imagery and data sets have been used in mine warfare applications but to a very minor extent and only at higher level. The usage should be increased and disseminated to the shipboard level so that captains and operations officers can better prepare for missions and complete them in a timelier manner.

Another comparison could be made between EO-1 and MODIS to see satellite vs. satellite differences. This comparison would have far reaching affects and may provide more insight into uses of satellite imagery.

### **C. SUGGESTIONS FOR FUTURE STUDY**

Due to timing, two years worth of hurricane season data could not be acquired (2006 hurricane season is not yet over). Follow on studies to determine and compare suspended sediment transport during hurricane seasons would be useful and informative for long-term seasonal sediment changes.

The potential capability to detect mines in coastal regions with a Hyperspectral imager is purely speculation based upon imagery available. A study using mine shapes would validate this hypothesis and be a great study. Coordination with the Mine Warfare Center in Panama City, Florida could make this a possibility.

For more direct comparisons of hyperspectral and multispectral imagery a larger water column sample must be evaluated. Gathering a hyperspectral image set that is not interrupted by the presence of land would allow further study of the limitations and similarities of each sensor. Data set sizes should be more equal as well. One set made up of over 340 samples and the other of only six samples (and one that is uninterrupted by land) is difficult to compare.

Shorter time series analysis would provide amplifying information about how current shifts affect the sediment transport. A one-week time series before and after each major storm event would provide more information also on how the sediment is traveling.



## LIST OF REFERENCES

- Gyory, Joanna, Rowe, Elizabeth, Mariano, Arthur J., Ryan, Edward H. "The Florida Current." Ocean Surface Currents. 2001-2005 Website:  
<http://oceancurrents.rsmas.miami.edu/atlantic/florida.html>. August 2006
- Kunte, P.D. Zhao, C. Osawa, T. Sugimori, Y. Sediment distribution study in the Gulf of Kachchh, India, from 3D hydrodynamic model simulation and satellite data. Journal of Marine Systems, 55, 139-153, 2005.
- Lee, ZhongPing., Carder, K. L., Arnone, R. A., Deriving Inherent Optical Properties From Water Color: A Multiband Quasi-analytical Algorithm for Optically Deep Waters, APPLIED OPTICS, Vol. 41, No. 27, 5755-5772, 2002.
- Li, Jun, Liu, Chian-Yi, Huang, H.L., Wu, Xuebao, Schmit, Timothy J., Menzel, W Paul., An optimal cloud-clearing method for AIRS radiances using MODIS, Cooperative Institute for Meteorological Satellite Studies, <http://cimss.ssec.wisc.edu/itwg/itsc/itsc14/proceedings/>, May 2006
- Martin, Seelye. An Introduction to Ocean Remote Sensing. Cambridge University Press 133-142, 187, 2004
- Melin, F., Zibordi, G., Berthon, J., Assessment of apparent and inherent optical properties derived from SeaWiFS with field data, Remote Sensing of Environment, 540-553, March 2005
- Miller, R.L., McKee, B.A., Using MODIS Terra 250m Imagery to Map Concentrations of Total Suspended Matter in Coastal Waters. Remote Sensing of Environment, 93, 259-266, July 2004
- Mobley, C.D., 1994: Light and Water Radiative Transfer in Natural Waters. Academic Press, 592
- Morel, A., Loisel, H., Apparent Optical Properties of Oceanic Water: Dependence on the Molecular Scattering Contribution. Applied Optics, Vol. 37, 4765-4776, 1998

- Museler, E.A., A Comparison of In-Situ Measurements and Satellite Remote Sensing of Underwater Visibility, Naval Postgraduate Thesis, Department of Meteorology and Physical Oceanography, 2003
- National Aeronautics and Space Administration (NASA), MODIS Web, website: <http://modis.gsfc.nasa.gov/>, September 2006.
- National Data Buoy Center (NDBC) 1100 Balch Blvd. Stennis Space Center, MS 39529: Website <http://www.ndbc.noaa.gov/>, September 2006.
- Natural Environment Research Council Airborne Research and Survey Facility (NERC ARSF), Instrument Specifications website: <http://arsf.nerc.ac.uk/>, 2005
- Preisendorfer, R.W., 1976: Hydrologic Optics. Vol. 1. U.S. Department of Commerce, 218 pp.
- Rainey, M.P. Tyler, A.N. Gilvear, D.J. Bryant, R.G. and McDonald, P. Mapping intertidal estuarine sediment grain size distributions through airborne remote sensing. Remote Sensing of Environment, 86, 480-490, 2003
- Roesler, Collin S., Boss, Emmanuel, A NOVEL REFLECTANCE INVERSION MODEL: Retrieval of Beam Attenuation Coefficients and Particle Size Distributions From Ocean Color, [www.bigelow.org/srs/Roesler\\_Boss\\_2002\\_00.pdf](http://www.bigelow.org/srs/Roesler_Boss_2002_00.pdf), 2002, 1-10 April, 2006.
- Ruhl, C.A. Schoellhamer, D.H. Stumpf, R.P. and Lindsay, C.L. Combined Use of Remote Sensing and Continuous Monitoring to Analyse the Variability of Suspended-Sediment Concentrations in San Francisco Bay, California. Estuarine, Coastal and Shelf Science, 53, 801-812, 2001.
- Smith, R.A, Irish, J.L, Smith, M.Q, Airborne Lidar and Airborne Hyperspectral Imagery: A Fusion of Two Proven Sensors for Improved Hydrographic Surveying, [http://shoals.sam.usace.army.mil/downloads/Publications/27Smith\\_Irish\\_Smith\\_00.pdf](http://shoals.sam.usace.army.mil/downloads/Publications/27Smith_Irish_Smith_00.pdf), April 2006.
- Smith, Randall B., Introduction to Hyperspectral Imaging with TNTmips®, <http://www.microimages.com>, August 2006

Stumpf, R.P. and Holderied, K. Deterimination of Water Depth with High-Resolution Satellite Imagery Over Variable Bottom Types. *Limnol. Oceanogr.*, 48, 547-556, 2003.

Twardowski, M.S., Boss, E., Macdonald, J.B., Pegau, W.S., Barnard, A.H., Zaneveld, J.R.V., A model for estimating bulk refractive index from the optical backscattering ratio and the implications for understanding particle composition in case I and case II waters, *Journal of Geophysical Research*, Vol. 106, 14129-14142, 2001.

University of California, Earth & Planetary Sciences 1156 High Street, Santa Cruz, CA 95064, Website: <http://www.es.ucsc.edu/>, September 2006.

THIS PAGE INTENTIONALLY LEFT BLANK

## INITIAL DISTRIBUTION LIST

1. Defense Technical Information Center  
Ft. Belvoir, Virginia
2. Dudley Knox Library  
Naval Postgraduate School  
Monterey, California
3. Mary Batteen, Chair (Code OC)  
Department of Oceanography  
Naval Postgraduate School  
Monterey, California
4. Don Brutzman, Chair (Code USW)  
Department of Undersea Warfare  
Naval Postgraduate School  
Monterey, California
5. Robin Tokamian (Code OC)  
Department of Oceanography  
Naval Postgraduate School  
Monterey, California
6. Rost Parsons  
Naval Research Lab  
Stennis Space Center, Mississippi